CHAPTER 14

ANALYSIS AND DESIGN BY COMPUTER OF PILES SUBJECTED TO LATERAL LOADING

14.1 NATURE OF THE COMPREHENSIVE PROBLEM

Chapter 12 demonstrated that the analysis and design of a pile under lateral loading requires the solution of a nonlinear problem in soil–structure interaction. The nonlinearity was reflected in the reduced value of a secant E_{py} to a *p*-*y* curve with pile deflection where *y* represents the lateral deflection and *p* represents the resistance from the soil in force per unit length.

A second nonlinearity must be addressed. The value of the bending stiffness E_pI_p of a reinforced concrete pile, in particular, will be reduced as the bending moment along the pile is increased. For a pile of reinforced concrete, explicit expressions must be developed, based on the geometry of the cross section of the pile and the properties of the steel and concrete, yielding the value of E_pI_p as a function of the applied bending moment. The method can be applied to piles with cross sections of other materials as well. Then a code must be written to determine the bending moment during a computation so that the value of E_pI_p can be modified as iterations proceed.

The differential equation for a pile under lateral loading given in Chapter 12 must be modified to account for the effect of axial loading on bending moment, sometimes called the $P - \Delta$ *effect.* The modified differential equation will allow the buckling of the pile under axial loading to be investigated, as well as account for the increased bending moment. The solution of the modified differential equation proceeds in a relatively straightforward way, using the power of the computer. Numerical techniques involving double-precision arithmetic are used, and the engineer must understand the nature

Copyright © 2006 John Wiley & Sons Retrieved from: www.knovel.com

of the numerical solutions to ensure that no computational errors occur due to improper selection of word length and computational tolerance during iterations.

The concept of *p-y* curves was presented in Chapter 12, and recommendations will be presented here on soils and rock under both static and repeated loading conditions. The recommendations are based on mechanics as much as possible but, more importantly, are based strongly on full-scale experiments in the field. Sustained loading will not cause much change in soil resistance for granular soil and overconsolidated clay. Field tests are recommended for piles in normally consolidated clay under sustained loading. In addition to specific recommendations for the formulation of *p-y* curves for soils and rock, several applications are presented for the solution of problems encountered in practice.

14.2 DIFFERENTIAL EQUATION FOR A COMPREHENSIVE SOLUTION

The differential equation required for a comprehensive solution is an expansion of Eq. 12.12 in Chapter 12. The two added features are the ability to account for an axial load and a distributed load. In many problems, the additional bending caused by an axial load is moderate but an important capability is added: computation of the load to cause buckling, particularly for piles that extend some distance above the groundline. The ability to consider a distributed force is essential in analyzing a pile extending through flowing water or subjected to pressures from moving earth. The differential equation for a comprehensive solution is

$$E_p I_p \frac{d^4y}{dx^4} + P_x \frac{d^2y}{dx^2} - p + W = 0 \tag{14.1}$$

where

P_x = axial load on the pile (positive to cause compression on the pile), and
W = distributed load in force per unit of length along the pile (positive in the positive direction of y).

The solution of Eq. 14.1 by numerical techniques is shown later in this chapter.

Copyrighted Material

Copyright © 2006 John Wiley & Sons Retrieved from: www.knovel.com

14.3 RECOMMENDATIONS FOR *p-y* CURVES FOR SOIL AND ROCK

14.3.1 Introduction

Basis for Useful Solutions The ability to make detailed analyses and a successful design of a pile to sustain lateral loading depends principally on the prediction of the response of the soil with appropriate accuracy. The computer gives the engineer the ability to solve complex nonlinear problems speedily, and with *p-y* curves for the soil and pile loadings, the differential equation can be solved with dispatch to investigate a number of parameters.

Prediction of the *p-y* curves for a particular solution must be given careful and detailed attention, starting with the acquisition of data on soils at the site, with particular reference to the role of water, use of soil mechanics to the extent possible, consideration of the nature of the loading at the site, evaluation of available data on performance of soils similar to those at the site, and development of multiple solutions to evaluate the importance of various parameters in the methods of prediction.

As shown in the following sections, the mechanics of soils have been used to gain information on the slope of the early portion of *p-y* curves and on the magnitude of the ultimate soil resistance p_u that develops with relatively large deflection of a pile. However, the performance of full-scale tests in the field with instrumented piles has been indispensable in the development of prediction methods.

Field Tests with Instrumented Piles The preferred method is to instrument a pile at close intervals along its length with electrical-resistance strain gauges for the measurement of bending moment as a series of measured loads are applied to the pile (Matlock and Ripperger, 1956). Integration of the bending moments from one of the loadings, using the boundary conditions, will yield values of y as a function of depth. Differentiation of the bending moments from the same loading, usually requiring special techniques, will yield values of p as a function of depth. Repeating the process for all of the loadings and cross-plotting values of p versus values of y will yield a family of *p-y* curves. The curves in Figure 12.3 were obtained by using the technique just described. There is considerable expense in the careful instrumentation of a pile, the installation at a site where data are needed, the performance of the test and the acquisition of data, and the analysis of the data. A limited number of such tests have been done.

A second experimental technique involves the steps noted above, except for installation of the internal instrumentation along the pile. Four boundary conditions are measured at the pile head for a series of loadings: deflection, slope, moment, and shear. Nondimensional techniques are employed, and val-

Copyrighted Material

Copyright © 2006 John Wiley & Sons Retrieved from: www.knovel.com

ues of E_{py} as a function of depth are found that will fit the measured data (Reese and Cox, 1968). Values of y and p are computed as a function of depth. The procedure is repeated for each of the applied loads; cross-plotting then yields a family of p-y curves.

The p-y curves from experiments were used to compute pile-head deflection as a function of applied load to compare with results from tests where limited data were obtained. Comparisons were possible only where relevant data were available on pile, loadings, and soil. Where comparisons could be made, the results were useful in validating the quality of p-y curves from tests of instrumented piles.

Characteristics of p-y Curves A typical p-y curve is shown in Figure 14.1a, drawn only in the first quadrant for convenience, and is meant to represent the case where a short-term monotonic loading, or "static" loading, is applied to a pile. The three curves in Figure 14.1 show a straight-line relationship between p and y from the origin to point a. Assuming that the strain of soil is linearly related to stress for small strains, the assumption follows that p is linearly related to y for small deflections. Analytical methods for establishing such a relationship are discussed later in this chapter.

The portion of the curve in Figure 14.1a from point a to point b shows that the value of p is increasing at a decreasing rate with respect to y. This

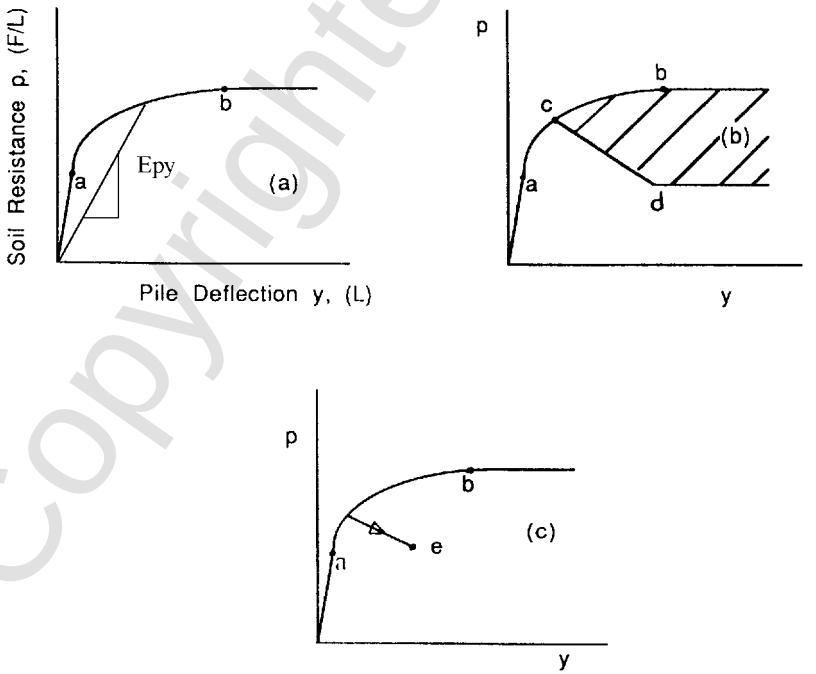

Figure 14.1 Conceptual p-y curves.

Copyrighted Material

Copyright © 2006 John Wiley & Sons Retrieved from: www.knovel.com

behavior reflects the nonlinear portion of the stress-strain curve for natural soil; no analytical method is currently available for computing the *a-b* portion of a *p-y* curve. The horizontal portion of the *p-y* curve in Figure 14.1a indicates that the soil is behaving plastically, with no loss of shear strength with increasing strain. Analytical models can be used to compute the ultimate resistance p_u as a function of pile dimensions and soil properties. These models will be demonstrated later in this chapter.

The shaded portion of the *p-y* curve shown in Figure 14.1b shows decreasing values of *p* from point *c* to point *d*. The decrease reflects the effect of cyclic loading. The curves in Figures 14.1a and 14.1b are identical up to point *c*, which implies that cyclic loading has little or no effect on a *p-y* curve for small deflections. The loss of resistance represented by the shaded area is, of course, related to the number of loading cycles. However, the number of cycles does not appear in the criteria shown later; rather, the assumption is made that the repeated loading is sufficient to cause the limiting value of soil resistance.

The possible effect of sustained loading is shown in Figure 14.1c, where there is an increase in *y* with a corresponding loss of *p*. For a pile in normally consolidated clay, lateral loading will cause an increase in porewater pressure and deflection will increase as the porewater pressure is dissipated. The decrease in the value of *p* suggests that resistance is shifted to other elements along the pile as deflection occurs at a particular point. A prediction of the effect of sustained loading for piles in soft or normally consolidated clays must be developed from field testing or estimated using the theory of consolidation. Sustained loading should have little effect on the behavior of piles in granular soils or in most overconsolidated clays.

Many soil profiles consist of a series of layers, with some, on occasion, being thin with respect to the diameter of the pile being designed. If relatively thin layers exist at a site, the engineer may wish to implement the method proposed by Georgiadis (1983).

Effects of Cyclic Loading Cyclic loading occurs in a number of designs; a notable example is an offshore platform. Therefore, a number of the field tests employing fully instrumented piles have used cyclic loading in the experimental procedures. Cyclic loading has invariably resulted in increased deflection and bending moment above the respective values obtained in short-term loading.

Cohesive Soils. A dramatic example of the loss of soil resistance due to cyclic loading may be seen by comparing the two sets of *p-y* curves in Figures 12.11a and 12.11b, where the pile was installed in overconsolidated clay with water being present above the ground surface. To gain information on the reasons for the dramatic loss of resistance shown in Figure 12.3b, Wang (1982) and Long (1984) did extensive studies of the influence of cyclic loading on *p-y* curves for clays. The following two reasons can be suggested for the reduction in soil resistance from cyclic loading: subjection of the clay to

Copyrighted Material

Copyright © 2006 John Wiley & Sons Retrieved from: www.knovel.com

repeated strains of large magnitude, with a consequent loss of shearing strength due to remolding, and scour from the enforced flow of water in the vicinity of the pile. Long studied the first factor by performing some triaxial tests with repeated loading using specimens from sites where piles had been tested. The second factor is present when water is above the ground surface, and its influence can be severe.

Welch and Reese (1972) reported some experiments with a bored pile under repeated lateral loading in an overconsolidated clay with no free water present. During cyclic loading, the deflection of the pile at the groundline was on the order of 25 mm (1 in.). After a load was released, a gap was revealed at the face of the pile where the soil had been pushed back. Also, cracks a few millimeters wide radiated away from the front of the pile. Had water covered the ground surface, it is evident that water would have penetrated the gap and the cracks. With the application of a load, the gap would have closed and the water carrying soil particles would have been forced to the ground surface. This process was dramatically revealed during soil testing in overconsolidated clay at Manor (Reese et al., 1975) and at Houston (O'Neill and Dunnavant, 1984).

While the work of Long (1984), Wang (1982), and others produced considerable information on the factors that influence the loss of resistance in clays under free water due to cyclic loading, it did not produce a definitive method for predicting this loss of resistance. The analyst thus should use the numerical results presented here with caution in regard to the behavior of piles in clay under cyclic loading. Full-scale experiments with instrumented piles at a particular site are indicated for those cases where behavior under cyclic loading is a critical feature of the design.

Cohesionless Soils. The loss of resistance of granular soil due to the cyclic lateral loading of piles is not nearly as dramatic for cohesionless soil as it is for clay soils. Cyclic loading will usually cause a change in the void ratio of the soil, which may result in settlement of the ground surface. If the pile is cycled in the same direction with loads that cause deflection of more than a few millimeters, the granular soil with no cohesion will collapse behind the pile and cause deflection to be ''locked in.''

The relative density of granular soils should be determined as accurately as possible prior to construction of piles to be subjected to lateral loading. If the soil is dense, driving the piles may be impossible and an alternative procedure for installation may be selected. If the soil is loose, densification will occur during pile driving, and further densification can occur during cyclic loading. The engineer will want to use all details on the soil and the response of the pile, from full-scale experiments of piles under lateral loading in granular soils, to use most effectively the information show later in predicting *p-y* curves for a particular design.

Influence of Diameter The analytical developments presented to this point indicate that the term for the pile diameter appears to the first power in the

Copyright © 2006 John Wiley & Sons Retrieved from: www.knovel.com

expressions for *p-y* curves. This idea is reinforced when the concept of a stress *bulb* is employed for piles under static loading. Elementary analysis shows that the ratio of load per unit length and the pile deflection would be the same for any diameter. However, cyclic loading of piles in clay below the water surface involves phenomena that are probably not related to diameter.

Some experimental studies have been done that provide useful information. Reese et al. (1975) described tests of piles with diameters of 152 mm (6 in.) and 641 mm (24 in.) at the Manor site. The *p-y* formulations developed from the results with the larger piles were used to analyze the behavior of the smaller piles. The computation of bending moment led to good agreement between analytical and experimental results, but the computation of groundline deflection showed considerable disagreement, with the computed deflections being smaller than the measured ones.

O'Neill and Dunnavant (1984) and Dunnavant and O'Neill (1986) reported on tests performed at a site where the clay was overconsolidated and where lateral loading tests were performed on piles with diameters of 273 mm (10.75 in.), 1220 mm (48 in.), and 1830 mm (72 in.). They found that the site-specific response of the soil could best be characterized by a nonlinear function of the diameter.

In the recommendations that follow for the formulation of *p-y* curves, the diameter b appears to the first power, which does not seriously contradict any available experimental data. However, for piles of large diameter in overconsolidated clay below the water table, further experimental studies are recommended.

14.3.2 Recommendations for *p-y* Curves for Clays

Initial Portion of Curves The conceptual *p-y* curves in Figure 14.1 are characterized by an initial straight line from the origin to point a. A mass of soil with an assumed linear relationship between compressive stress and strain $E_{s\max}$ for small strains can be considered, where $E_{s\max}$ is the slope of the initial portion of the stress-strain curve in the laboratory. If a pile is made to deflect a small distance in such a soil, one can assume that the principles of mechanics can be used to find the initial slope K_{py} of the *p-y* curve. These are some difficulties in making the computations.

For one thing, the value of $E_{s\max}$ for soil is not easily determined. Stress-strain curves from unconfined compression tests were studied (Figure 14.2), and it was found that the initial modulus $E_{s\max}$ ranged from about 40 to about 200 times the undrained shear strength c (personal files). There is a considerable amount of scatter in the points, probably due to the heterogeneity of the soils at the two sites. The values of $E_{s\max}/c$ would probably have been higher had an attempt been made to get precise values for the early part of the curve. Stokoe (1989) reported that values of $E_{s\max}$ on the order of 2000 times c are found routinely in laboratory tests when soil specimens are subjected to very small strains. Johnson (1982) performed some tests with the self-boring pressuremeter, and computations with his results gave values of

Copyrighted Material

Copyright © 2006 John Wiley & Sons Retrieved from: www.knovel.com

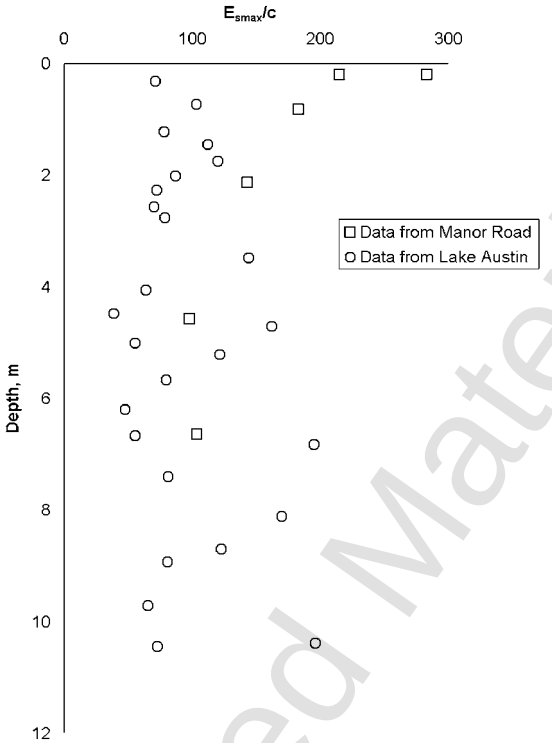

Figure 14.2 Plot of ratio of modulus to undrained shear strength from unconfined-compression test of specimens of clay.

$E_{s\max}/c$ that ranged from 1440 to 2840, with an average of 1990. The studies of the initial modulus from compressive stress-strain curves of clay seem to indicate that such curves are linear only over a very small range of strains.

The theory of elasticity (Vesić, 1961) and FEM (Yegian and Wright, 1973; Thompson, 1977; Kooijman, 1989; Brown et al., 1989) have been used to find values of $K_{py\max}$, the largest value of $K_{py\max}$, as a function of $E_{s\max}$ with limited success. With both methods, the presence of the ground surface presents analytical problems and no method of analysis can, at present, deal with the phenomena associated with cyclic loading, particularly if water is present at the ground surface. Considering the experimental difficulties in getting good values of $E_{s\max}$ and the analytical difficulties in obtaining values of $K_{py\max}$, the current best approach is to use values for the initial slope of p-y curves from experiments where careful controls were used. An example of such data is shown in Figure 14.3 (Reese et al., 1975). Table 14.1 was compiled after examining such data from experiments with a number of instrumented piles.

Ultimate Resistance p_u for Clays Two models can be used to gain some insight into the ultimate resistance p_u that will develop as a pile is deflected

Copyright © 2006 John Wiley & Sons Retrieved from: www.knovel.com

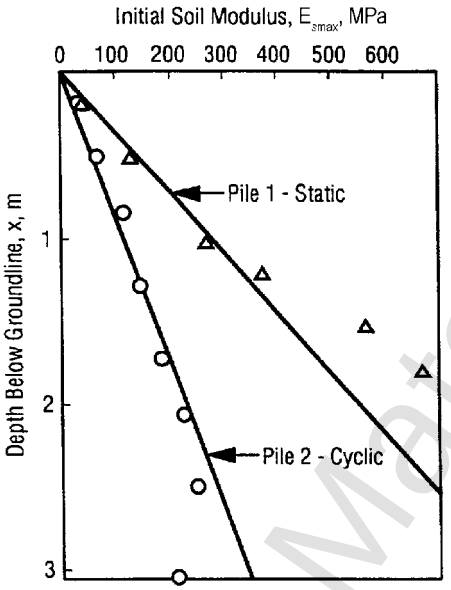

Figure 14.3 Initial soil modulus versus depth.

laterally. The first model assumes that the clay will move up and out at the ground surface; the second model takes over below the first and assumes horizontal movement of the clay. A wedge of soil for the first model is shown in Figure 14.4. Justification for the use of this model is presented in Figures 14.5a and 14.5b (Reese et al., 1975), where contours are shown of the rise of the ground surface at the front of a steel-pipe pile with a diameter of 641 mm (24 in.) in overconsolidated clay. As shown in Figure 14.5a, for a lateral load of 596 kN (134 kips), ground-surface movement occurred at a distance from the axis of the pile of about 4 m (13 ft). When the load was removed, the ground surface subsided somewhat, as shown in Figure 14.5b, suggesting that the soil behaved plastically.

TABLE 14.1 Representative Values of K_{py} for Clays

	Average Undrained Shear Strength*		
kPa	50–100	200–300	300–400
K_{py} (static) MN/m^3	135	270	540
(lb/in.^{3})	(500)	(1000)	(2000)
K_{py} (cyclic) MN/m^3	55	110	540
(lb/in.^{3})	(200)	(400)	(2000)

*The average shear strength should be computed to a depth of five pile diameters. It should be defined as half of the total maximum principal stress difference in an unconsolidated, undrained triaxial test.

Copyrighted Material

Copyright © 2006 John Wiley & Sons Retrieved from: www.knovel.com

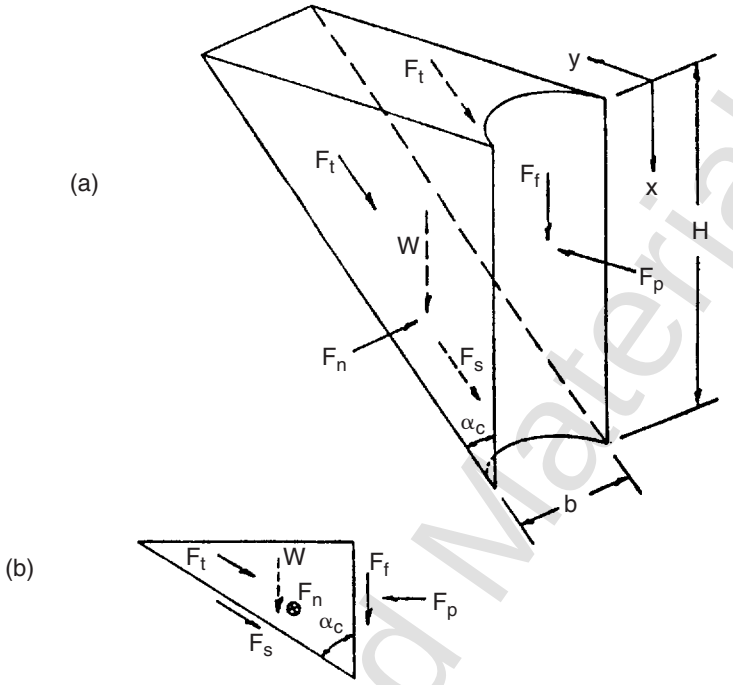

Figure 14.4 Assumed passive wedge-type failure for clay: (a) shape of the wedge; (b) forces acting on the wedge.

The use of plane sliding surfaces, shown in Figure 14.4, will obviously not model the movement indicated by the contours in Figure 14.5; however, a solution with the simplified model should give some insight into the variation of the ultimate lateral resistance p_u with depth. Taking the weight of the wedge into account, taking for the forces on the sliding surfaces into account, solving for F_p, and differentiating F_p with respect to H to solve for p_{u1} leads to Eq. 14.2:

$$p_{u1} = c_a b[\tan \alpha_c + (1 + \kappa)\cot \alpha_c] + \gamma bH + 2c_a H(\tan \alpha_c \sin \alpha_c + \cos \alpha_c) \tag{14.2}$$

where

p_{u1} = ultimate resistance near the ground surface per unit of length along the pile,
c_a = average undrained shear strength over the depth H,
α_c = angle of the inclined plane with the vertical,
γ = unit weight of soil, and
κ = reduction factor for shearing resistance along the face of the pile.

Copyrighted Material

Copyright © 2006 John Wiley & Sons Retrieved from: www.knovel.com

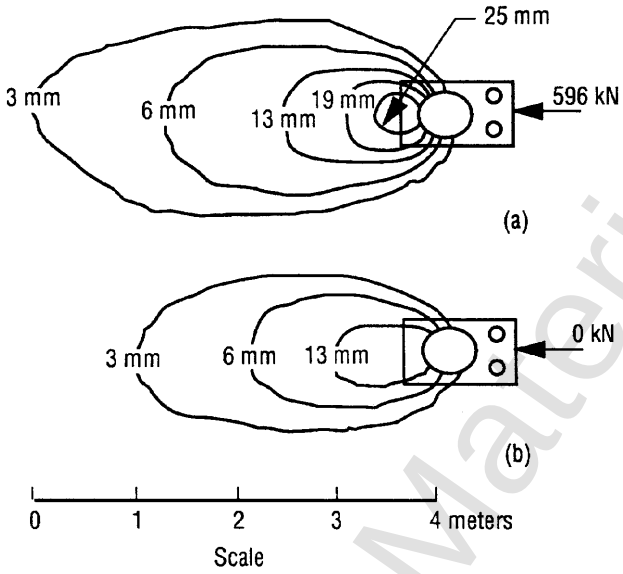

Figure 14.5 Ground heave due to static loading of pile 1: (a) heave at the maximum level; (b) residual heave.

If κ is set equal to zero, which is logical for the case of cyclic loading, and α_c is set at 45°, the following equation results:

$$p_{u1} = 2c_a b + \gamma bH + 2.83c_a H \tag{14.3}$$

The second model for computing the ultimate resistance p_u is shown in the plan view in Figure 14.6. At some point below the ground surface the maximum value of soil resistance will occur, with the soil moving horizontally. Movement in only one side of the pile is indicated, but movement, of course, will be around both sides of the pile. Again, planes are assumed for the sliding surfaces, with the acceptance of some approximation in the results.

A cylindrical pile is indicated in Figure 14.6, but for convenience in computation, a prismatic block of soil is assumed to be subjected to horizontal movement. Block 5 is moved laterally, as shown, and stress of sufficient magnitude is generated in that block to cause failure. Stress is transmitted to Block 4 and on around the pile to Block 1, with the assumed movements indicated by the dotted lines. Block 3 is assumed not to distort, but failure stresses develop on the sides of the block as it slides.

The Mohr-Coulomb diagram for undrained, saturated clay is shown in Figure 14.6b, and a free body of the pile is shown in Figure 14.6c. The ultimate soil resistance p_{c2} is independent of the value of σ_1 because the difference in the stress on the front σ_6 and back σ_1 of the pile is equal to $10c$. The shape of the cross section of a pile will have some influence on the magnitude of

Copyrighted Material

Copyright © 2006 John Wiley & Sons Retrieved from: www.knovel.com

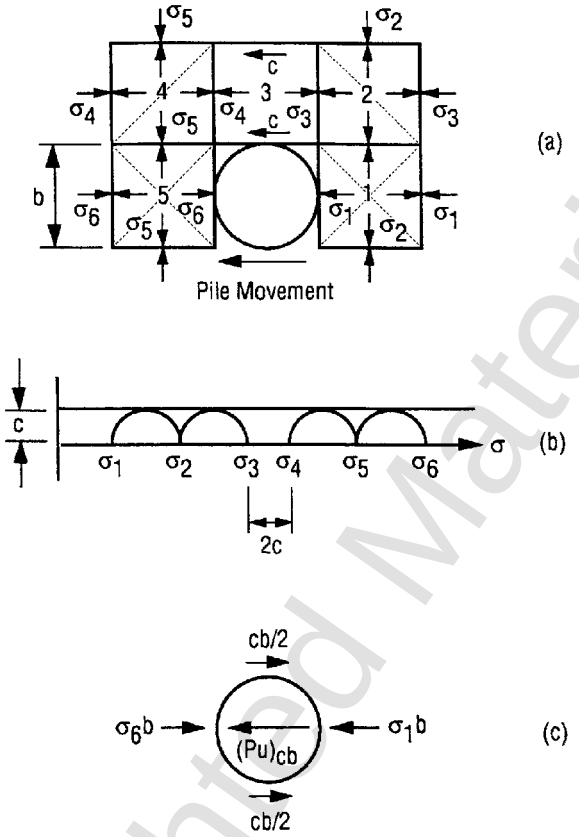

Figure 14.6 Assumed mode of soil failure by lateral flow around a pile in clay: (a) section through the pile; (b) Mohr-Coulomb diagram; (c) forces acting on a section of a pile.

p_{u2} for the circular cross section. It is assumed that the resistance developed on each side of the pile is equal to $cb/2$, and

$$p_{u2} = (\sigma_6 - \sigma_1 + c)\, b = 11cb \tag{14.4}$$

Equations 14.3 and 14.4 are similar to equations shown later in the recommendations for two of the sets of *p-y* curves. However, emphasis is placed directly on experimental results. The elementary analytical procedures shown here give considerable guidance to the recommendations that follow, but the results from experiments, similar in form to the above results, were favored. Note that many cases were analyzed where available data allowed the results of experiments to be compared with analytical results, confirming the value of the methods shown below.

Copyrighted Material

Copyright © 2006 John Wiley & Sons Retrieved from: www.knovel.com

Early Recommendations Designers used all available information in selecting the sizes of piles to sustain lateral loading in the period prior to the advent of instrumentation that allowed the development of *p-y* curves from experiments with instrumented piles. The methods yielded soil modulus values that were employed principally with closed-form solutions of the differential equation. The work of Skempton (1951) and the method proposed by Terzaghi (1955) were useful to early designers.

The method proposed by McClelland and Focht (1958), outlined below, appeared at the beginning of the period when large research projects were funded and is significant because those authors were the first to present the concept of *p-y* curves. Their paper is based on a full-scale experiment at an offshore site where a moderate amount of instrumentation was employed. Because the test was at an offshore site, rigorous control of the experiment was not possible. The paper shows conclusively that soil modulus is not a soil property but instead is a function of pile deflection and depth below the mudline, as well as of soil properties.

The paper recommends the performance of consolidated-undrained triaxial tests with the confining pressure equal to the overburden pressure. The full curve of compressive stress σ_1 and the corresponding strain ε is plotted. The following equation is recommended for obtaining the value of soil resistance p:

$$p = 5.5\sigma_1 b \tag{14.5}$$

To obtain values of the corresponding pile deflection y from stress-strain curves, the authors proposed the following equation:

$$y = 0.5\varepsilon b \tag{14.6}$$

The McClelland-Focht equations resemble the more comprehensive equations developed from tests of instrumented piles, shown below, except for the reduction in the value of p near the ground surface. The recommendations in the following three sections are currently used in many designs.

Response of Soft Clay in the Presence of Free Water Matlock (1970) performed lateral-load tests with a steel-pipe pile that was 324 mm (13 in.) in diameter and 12.8 m (42 ft) long. It was driven into clays near Lake Austin, Texas, that had a shear strength averaging about 38 kPa (800 lb/ft^2). The pile was recovered, taken to Sabine Pass, Texas, and driven into clay with a shear strength that averaged about 14.4 kPa (300 lb/ft^2) in the significant upper zone.

The initial loading was short-term (static), but the load remained on the pile long enough for readings of strain gauges to be taken by an extremely precise device; however, some creep occurred at the higher loads. The two sets of readings at each point along the pile were interpreted to find the

Copyrighted Material

Copyright © 2006 John Wiley & Sons Retrieved from: www.knovel.com

assumed reading at a particular time, assuming that the change in moment due to creep was minor or had a constant rate. The accurate readings of bending moment allowed the soil resistance to be found by numerical differentiation.

The pile was extracted and redriven, and cyclic loading was applied. Readings of the strain gauges were taken under constant load after various numbers of loading cycles. The load was applied in two directions, with the load in the forward direction being more than twice as large as the load in the backward direction. After a significant number of cycles, the deflection at the top of the pile was changing not at all or only a small amount, and an equilibrium condition was assumed. Therefore, the *p-y* curves for cyclic loading are intended to represent a lower-bound condition.

The following procedure is for short-term static loading and is illustrated in Figure 14.7a. As noted earlier, the curves for static loading constitute the basis for indicating the influence of cyclic loading and would be used in design in special cases.

1. Obtain the best possible estimate of the variation of undrained shear strength c and submerged unit weight with depth. Also, obtain the value of ε_{50}, the strain corresponding to one-half of the maximum principal stress difference. If no stress-strain curves are available, typical values of ε_{50} are given in Table 14.2.

2. Compute the ultimate soil resistance per unit length of pile, using the smaller of the values given by the following equations:

$$p_u = \left[3 + \frac{\gamma'}{c} + \frac{J}{b}z\right]cb \tag{14.7}$$

$$p_u = 9cb \tag{14.8}$$

where

γ' = average effective unit weight from ground surface to *p-y* curve,
z = depth from ground surface to *p-y* curve,
c = undrained shear strength at depth z,
b = diameter (width) of pile, and
J = experimentally determined parameter.

Matlock (1970) stated that the value of J was determined to be 0.5 for a soft clay and about 0.25 for a medium clay. The value of 0.5 is frequently used for J. The value of p_u is computed at each depth where a *p-y* curve is desired based on shear strength at that depth.

3. Compute the deflection y_{50} at one-half of the ultimate soil resistance from the following equation:

Copyright © 2006 John Wiley & Sons Retrieved from: www.knovel.com

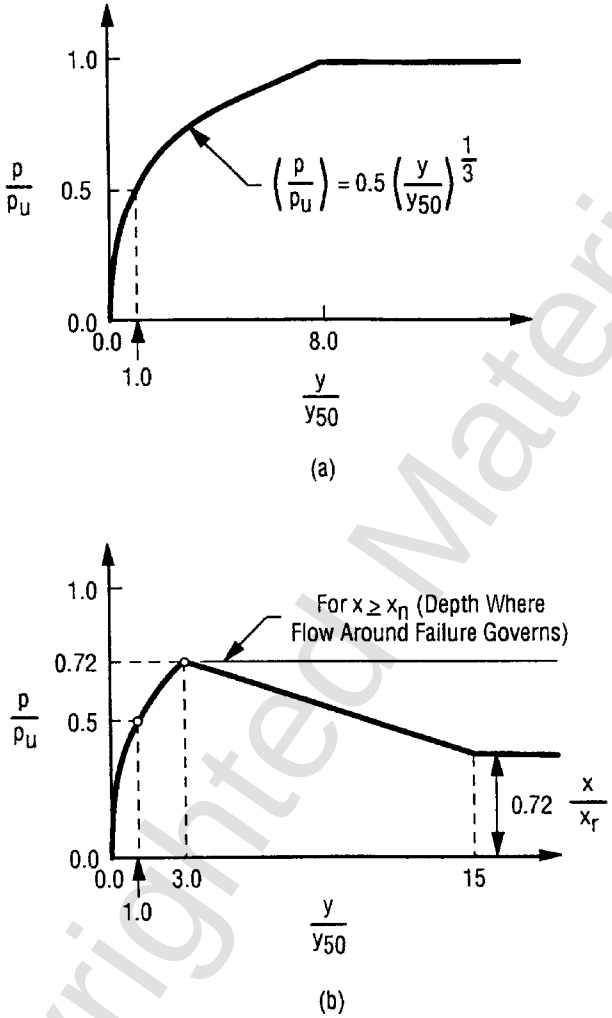

Figure 14.7 Characteristic shapes of *p-y* curves for soft clay in the presence of free water: (a) static loading; (b) cyclic loading (after Matlock, 1970).

TABLE 14.2 Representative Values of ε_{50}

Consistency of Clay, psf	Undrained Shear Strength, kPa	ε_{50}
Very soft	>250	>12	0.02
Soft	250–500	12–24	0.02
Medium	500–1000	24–48	0.01
Stiff	1000–2000	48–96	0.006
Very stiff	2000–4000	96–192	0.005
Hard	<2000	<192	0.004

Copyrighted Material

Copyright © 2006 John Wiley & Sons Retrieved from: www.knovel.com

$$y_{50} = 2.5\varepsilon_{50}b \tag{14.9}$$

4. Compute points describing the *p-y* curve from the following relationship:

$$\frac{p}{p_u} = 0.5\left(\frac{y}{y_{50}}\right)^{1/3} \tag{14.10}$$

The value of p remains constant beyond $y = 8y_{50}$. Equation 14.10 shows the slope of the *p-y* curve to be infinite at the origin, an anomalous result. The reasonable suggestion is made that the initial slope of the *p-y* curve be established by using K_{py} from Table 14.1.

With the modification shown above, the *p-y* curve for cyclic loading may be formulated by using the following procedure, illustrated in Figure 14.7b.

1. Construct the *p-y* curve in the same manner as for short-term static loading for values of p less than $0.72p_u$.
2. Solve Eqs. 14.7 and 14.8 simultaneously, taking the variation of c and γ' into account, to find the depth z_r where the transition occurs.
3. If the depth to the *p-y* curve is greater than or equal to z_r, select p as $0.72p_u$ for all values of y greater than $3y_{50}$.
4. If the depth of the *p-y* curve is less than z_r, note that the value of p decreases to $0.72p_u$ at $y = 3y_{50}$ and to the value given by the following expression at $y = 15y_{50}$:

$$p = 0.72p_u\left(\frac{z}{z_r}\right) \tag{14.11}$$

The value of p remains constant beyond $y = 15y_{50}$.

Response of Stiff Clay in the Presence of Free Water Reese et al. (1975) performed lateral-load tests with steel-pipe piles that were 641 mm (24 in.) in diameter and 15.2 m (50 ft) long. The piles were driven into stiff clay at a site near Manor, Texas. The clay had an undrained shear strength ranging from about 96 kPa (1 ton/ft^2) at the ground surface to about 290 kPa (3 ton/ft^2) at a depth of 3.7 m (12 ft).

The loading of the pile was carried out in a manner similar to that described for the tests performed by Matlock. A significant difference was that a data acquisition system was employed that allowed a full set of readings of the strain gauges to be taken in about 1 minute. Thus, the creep of the piles under sustained loading was small or negligible. The disadvantage of the system was that the accuracy of the curves of bending moment was such that curve fitting was necessary in doing the differentiations.

Copyrighted Material

Copyright © 2006 John Wiley & Sons Retrieved from: www.knovel.com

Also, as in the Matlock test recommendations for cyclic loading, the lower-bound case is presented. Cycling was continued until the deflection and bending moments appeared to stabilize. The number of loading cycles was on the order of 100, and 500 cycles were applied in a reloading test. During the experiment with repeated loading, a gap developed between the soil and the pile after deflection at the ground surface of perhaps 10 mm (0.4 in.), and scour of the soil at the face of the pile began at that time. There is reason to believe that scour would be initiated in overconsolidated clays after a given deflection at the mudline rather than at a given fraction of the pile diameter. However, the data available at present do not allow any change in the recommended procedures. But analysts could well recommend a field test at a particular site in recognition of some uncertainty regarding the influence of scour on *p-y* curves for overconsolidated clays.

The following procedure is for short-term static loading and is illustrated in Figure 14.8. As before, these curves form the basis for evaluating the effect of cyclic loading. They may also be used for sustained loading in some circumstances.

1. Obtain values of undrained shear strength c, soil submerged unit weight γ', and pile diameter b.
2. Compute the average undrained shear strength c_a over the depth z.
3. Compute the ultimate soil resistance per unit length of pile using the smaller of the values given by the following equations:

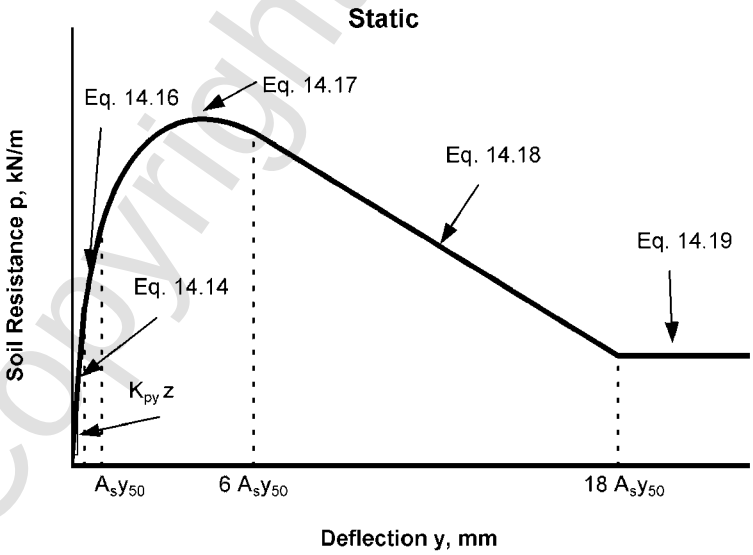

Figure 14.8 Characteristic shape of *p-y* curves for static loading in stiff clay in the presence of free water.

Copyrighted Material

Copyright © 2006 John Wiley & Sons Retrieved from: www.knovel.com

$$p_{ct} = 2c_a b + \gamma' bz + 2.83c_a z \tag{14.12}$$

$$p_{cd} = 11cb \tag{14.13}$$

4. Choose the appropriate value of A_s from Figure 14.9 for shaping the p-y curves.
5. Establish the initial straight-line portion of the p-y curve:

$$p = (K_{py}\, z)y \tag{14.14}$$

Use the appropriate value of K_{py} from Table 14.1.

6. Compute the following:

$$y_{50} = \varepsilon_{50} b \tag{14.15}$$

Use an appropriate value of ε_{50} from results of laboratory tests or, in the absence of laboratory tests, from Table 14.2.

7. Establish the first parabolic portion of the p-y curve, using the following equation and obtaining p_c from Eqs. 14.12 or 14.13:

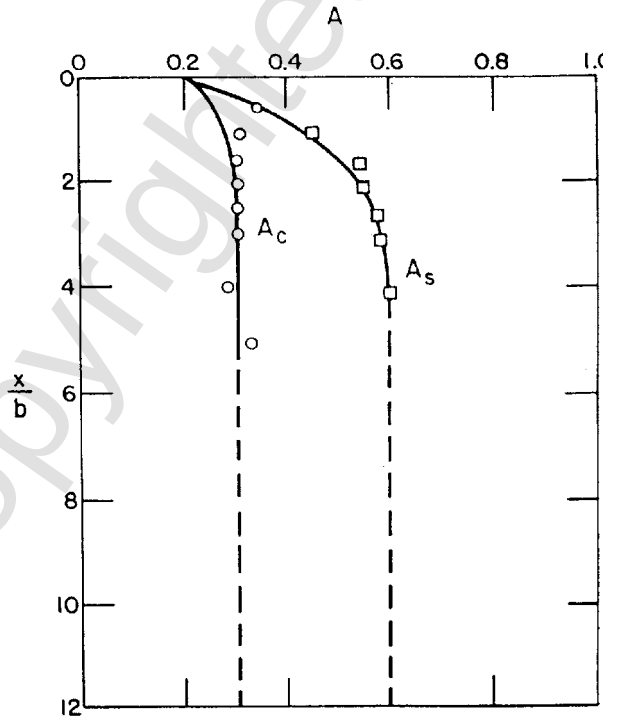

Figure 14.9 Values of constants A_s and A_c.

Copyrighted Material

Copyright © 2006 John Wiley & Sons Retrieved from: www.knovel.com

$$p = 0.5p_c\left(\frac{y}{y_{50}}\right)^{0.5} \tag{14.16}$$

Equation 14.16 should define the portion of the *p-y* curve from the point of the intersection with Eq. 14.14 to a point where y is equal to $A_s y_{50}$ (see the note in Step 10).

8. Establish the second parabolic portion of the *p-y* curve:

$$p = 0.5p_c\left(\frac{y}{y_{50}}\right)^{0.5} - 0.055p_c\left(\frac{y - A_s y_{50}}{A_s y_{50}}\right)^{1.25} \tag{14.17}$$

Equation 14.17 should define the portion of the *p-y* curve from the point where y is equal to $A_s y_{50}$ to a point where y is equal to $6A_s y_{50}$ (see note in Step 10).

9. Establish the next straight-line portion of the *p-y* curve:

$$p = 0.5p_c(6A_s)^{0.5} - 0.411p_c - \frac{0.0625}{y_{50}}p_c(y - 6A_s y_{50}) \tag{14.18}$$

Equation 14.18 should define the portion of the *p-y* curve from the point where y is equal to $6A_s y_{50}$ to a point where y is equal to $18A_s y_{50}$ (see the note in Step 10).

10. Establish the final straight-line portion of the *p-y* curve:

$$p = p_c[1.225(A_s)^{0.5} - 0.75A_s - 0.411] \tag{14.19}$$

Equation 14.19 should define the portion of the *p-y* curve from the point where y is equal to $18A_s y_{50}$. For all larger values of y, see the following note.

Note: The step-by-step procedure is outlined, and Figure 14.8 is drawn, as if there is an intersection between Eqs. 14.14 and 14.16. However, there may be no intersection of Eq. 14.14 with any of the other equations defining the *p-y* curve. Equation 14.14 defines the *p-y* curve until it intersects with one of the other equations; if no intersection occurs, Eq. 14.14 defines the complete *p-y* curve.

A second pile, identical to the pile used for static loading, was tested under cyclic loading. The following procedure is for cyclic loading and is illustrated in Figure 14.10. As may be seen from a study of the recommended *p-y* curves, the results for the Manor site showed a very large loss of soil resistance. The test data have been studied carefully, and the recommended *p-y* curves for cyclic loading reflect accurately the behavior of the soil at the site. Nevertheless, the loss of resistance due to cyclic loading at Manor is much greater than has been observed elsewhere. Therefore, use of the recommendations in this section for cyclic loading will yield conservative results for many clays.

Copyrighted Material

Copyright © 2006 John Wiley & Sons Retrieved from: www.knovel.com

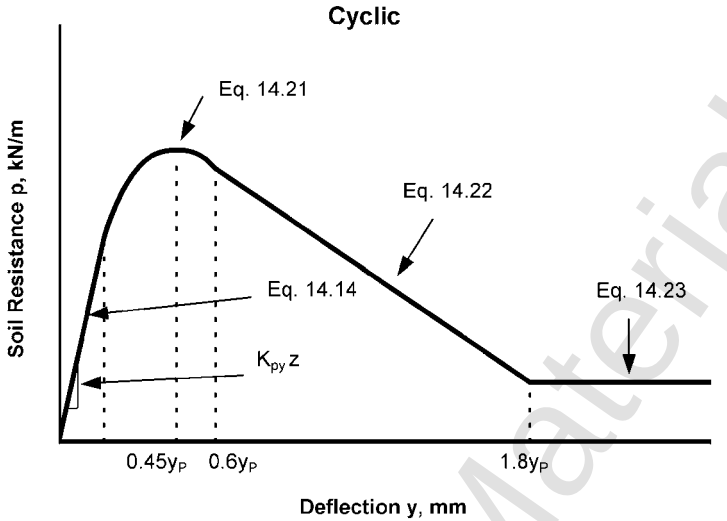

Figure 14.10 Characteristic shape of the *p-y* curve for cyclic loading in stiff clay in the presence of free water.

Long (1984) was unable to show precisely why the loss of resistance occurred during cyclic loading. One clue was that the clay from Manor was found to lose volume by slaking when a specimen was placed in fresh water. Thus, the clay was quite susceptible to erosion from the hydraulic action of the free water as the pile was pushed back and forth.

1. Steps 1, 2, 3, 5, and 6 are the same as for the static case.
4. Choose the appropriate value of A_c from Figure 14.9 for the particular nondimensional depth. Compute the following:

$$y_p = 4.1A_c y_{50} \tag{14.20}$$

7. Establish the parabolic portion of the *p-y* curve:

$$p = A_c p_c \left[1 - \left| \frac{y - 0.45y_p}{0.45y_p} \right|^{2.5} \right] \tag{14.21}$$

Equation 14.21 should define the portion of the *p-y* curve from the point of the intersection with Eq. 14.14 to where y is equal to $0.6y_p$ (see the note in Step 9).

8. Establish the next straight-line portion of the *p-y* curve:

$$p = 0.936A_c p_c - \frac{0.085}{y_{50}} p_c(y - 0.6y_p) \tag{14.22}$$

Copyrighted Material

Copyright © 2006 John Wiley & Sons Retrieved from: www.knovel.com

Equation 14.22 should define the portion of the *p-y* curve from the point where y is equal to $0.6y_p$ to the point where y is equal to $1.8y_p$ (see the note in Step 9).

9. Establish the final straight-line portion of the *p-y* curve:

$$p = 0.936A_c p_c - \frac{0.102}{y_{50}} p_c y_p \tag{14.23}$$

Equation 14.23 should define the portion of the *p-y* curve from the point where y is equal to $1.8y_p$ and for all larger values of y (see the following note).

Note: The step-by-step procedure is outlined, and Figure 14.10 is drawn, as if there is an intersection between Eq. 14.14 and Eq. 14.21. There may be no intersection of Eq. 14.14 with any of the other equations defining the *p-y* curve. If there is no intersection, the equation should be employed that gives the smallest value of p for any value of y.

Triaxial compression tests of the unconsolidated-undrained type with confining pressures conforming to in situ pressures are recommended for determining the shear strength of the soil. The value of ε_{50} should be taken as the strain during the test corresponding to the stress equal to one-half of the maximum total-principal-stress difference. The shear strength c should be interpreted as one-half of the maximum total-principal-stress difference. Values obtained from triaxial tests might be somewhat conservative but would represent more realistic strength values than values obtained from other tests. The unit weight of the soil must be determined.

Response of Stiff Clay with No Free Water A lateral-load test was performed at a site in Houston with a bored pile 915 mm (36 in.) in diameter. A 254-mm (10-in.)-diameter pipe, instrumented in intervals along its length with electrical-resistance-strain gauges, was positioned along the axis of the pile before concrete was placed. The embedded length of the pile was 12.8 m (42 ft). The average undrained shear strength of the clay in the upper 6 m (20 ft) was approximately 105 kPa (2200 lb/ft^2). The experiments and the interpretations are discussed by Welch and Reese (1972) and Reese and Welch (1975).

The same experiment was used to develop both the static and cyclic *p-y* curves, in contrast to the procedures employed for the two other experiments with piles in clays. The load was applied in only one direction, also in contrast to the other experiments.

A load was applied and maintained until the strain gauges were read with a high-speed data acquisition system. The same load was then cycled several times and held constant while the strain gauges were read at specific numbers of cycles. The load was then increased, and the procedure was repeated. The difference in the magnitude of successive loads was relatively large, and the

Copyrighted Material

Copyright © 2006 John Wiley & Sons Retrieved from: www.knovel.com

assumption was made that cycling at the previous load did not influence the readings for Cycle 1 at the new load.

The *p-y* curves at this site were relatively regular in shape, and yielded to an analysis that allowed the increase in deflection due to cyclic loading to be formulated in terms of the stress level and the number of loading cycles. Thus, the analyst can specify a number of loading cycles in doing the computations for a particular design.

The following procedure is for short-term static loading and is illustrated in Figure 14.11.

1. Obtain values for undrained shear strength c, soil unit weight γ, and pile diameter b. Also obtain the values of ε_{50} from stress-strain curves. If no stress-strain curves are available, use a value of ε_{50} as given in Table 14.2.
2. Compute the ultimate soil resistance p_u per unit length of pile using the smaller of the values given by Eqs. 14.7 and 14.8. (In using Eq. 14.7, the shear strength is taken as the average from the ground surface to the depth being considered and J is taken as 0.5. The unit weight of the soil should reflect the position of the water table.)
3. Compute the deflection y_{50} at one-half of the ultimate soil resistance from Eq. 14.9.
4. Compute points describing the *p-y* curve from the following relationship:

$$\frac{p}{p_u} = 0.5\left(\frac{y}{y_{50}}\right)^{0.25} \tag{14.24}$$

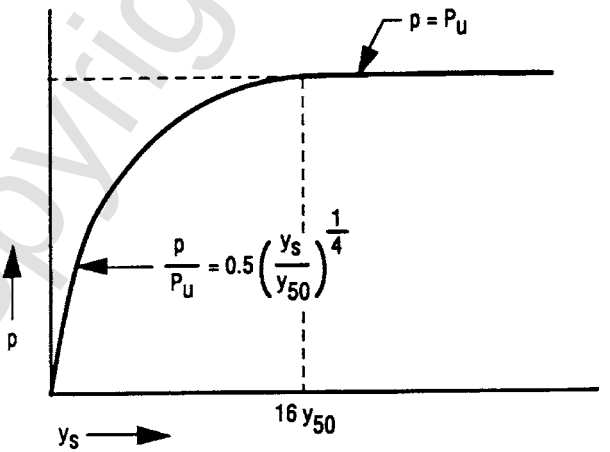

Figure 14.11 Characteristic shape of the *p-y* curve for static loading in stiff clay with no free water.

Copyrighted Material

Copyright © 2006 John Wiley & Sons Retrieved from: www.knovel.com

5. Beyond $y = 18y_{50}$, p is equal to p_u for all values of y.

The following procedure is for cyclic loading and is illustrated in Figure 14.12.

1. Determine the *p-y* curve for short-term static loading by the procedure previously given.
2. Determine the number of times the lateral load will be applied to the pile.
3. Obtain the value of C for several values of p/p_u, where C is the parameter describing the effect of repeated loading on deformation. The value of C is found from a relationship developed by laboratory tests (Welch and Reese, 1972) or, in the absence of tests, from the following equation:

$$C = 9.6\left(\frac{p}{p_u}\right)^4 \tag{14.25}$$

4. At the value of p corresponding to the values of p/p_u selected in Step 3, compute new values of y for cyclic loading from the following equation:

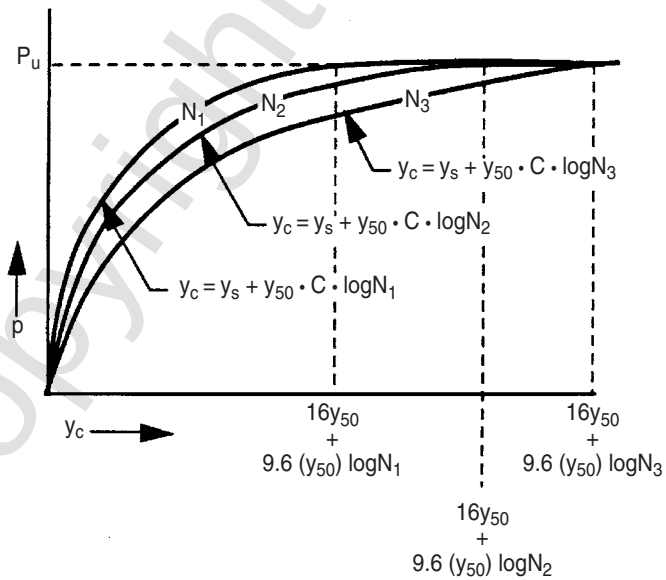

Figure 14.12 Characteristic shape of the *p-y* curve for cyclic loading in stiff clay with no free water.

Copyrighted Material

Copyright © 2006 John Wiley & Sons Retrieved from: www.knovel.com

$$y_c = y_s + y_{50} C \log N \tag{14.26}$$

where

y_c = deflection under N cycles of load,
y_s = deflection under short-term static load,
y_{50} = deflection under short-term static load at one-half of the ultimate resistance, and
N = number of cycles of load application.

5. The *p-y* curve defines the soil response after N cycles of loading.

The properties of the clay at the site should be obtained by triaxial compression tests of the unconsolidated-undrained type with confining stresses equal to the overburden pressures at the elevations from which the samples were taken to determine the shear strength. The value of ε_{50} should be taken as the strain during the test corresponding to the stress equal to one-half of the maximum total-principal-stress difference. The undrained shear strength c should be defined as one-half of the maximum total-principal-stress difference. The unit weight of the soil must also be determined.

14.3.3 Recommendations for *p-y* Curves for Sands

Initial Portion of Curves The initial stiffness of stress-strain curves for sand is a function of the confining pressure; therefore, the use of mechanics for obtaining $E_{py\max}$ for sands is complicated. The *p-y* curve at the ground surface will be characterized by zero values of p for all values of y, and the initial slope of the curves and the ultimate resistance will increase approximately linearly with depth.

The recommendations for the initial portion of the *p-y* curves for sand were derived principally from the results of experiments. As noted later, Terzaghi (1955) presented values that were useful in form, that is, starting with zero at the groundline and increasing linearly with depth. However, his values were for the case where the computed value of p would be equal to one-half of the ultimate bearing stress. Experimental results led to the recommendations in Table 14.3.

Ultimate Resistance p_u for Sands Two models are used for computing the ultimate resistance for piles in sand, following a procedure similar to that used for clay. The first model for the soil resistance near the ground surface is shown in Figure 14.13. The total lateral force F_{pt} (Figure 14.13c) may be computed by subtracting the active force F_a, computed by using Rankine theory, from the passive force F_p, computed from the model by assuming that the Mohr-Coulomb failure condition is satisfied on planes, *ADE*, *BCF*, and

Copyrighted Material

Copyright © 2006 John Wiley & Sons Retrieved from: www.knovel.com

TABLE 14.3 Representative Values of K_{py} for Sands

Relative Density of Sand	Loose	Medium	Dense
	Submerged Sand		
MN/m^3	5.4	16.3	34.0
psi	20.0	60.0	125.0
	Sand Above Water Table		
MN/m^3	6.8	24.4	61.0
psi	25.0	90.0	225.0

AEFB (Figure 14.13a). The directions of the forces are shown in Figure 14.13b. Solutions other than the ones shown here have been developed by assuming a friction force on the surface *DEFC* (assumed to be zero in the analysis shown here) and by assuming the water table to be within the wedge (the unit weight is assumed to be constant in the analysis shown here).

The force F_{pt} may be computed by following a procedure similar to that used to solve the equation in the clay model (Figure 14.4). The resulting equation is as follows:

$$F_{pt} = \gamma H^2\left[\left(\frac{K_0 H \tan\phi \tan\beta}{3\tan(\beta-\phi)\cos\alpha_s}\right) + \left(\frac{\tan\beta}{\tan(\beta-\phi)}\left(\frac{b}{2} + \frac{H}{3}\tan\beta\tan\alpha_s\right)\right)\right] + \gamma H^2\left[\frac{K_0 H\tan\beta}{3}(\tan\varphi\sin\beta - \tan\alpha_s) - \frac{K_A b}{2}\right] \quad (14.27)$$

where

ϕ = friction angle,
K_0 = coefficient of earth pressure at rest, and
K_A = minimum coefficient of active earth pressure = $\tan^2(45 - \phi/2)$.

Sowers and Sowers (1970) have recommended K_0 values of 0.6 for loose sand and 0.4 for dense sand.

The ultimate soil resistance near the ground surface per unit length of the pile is obtained by differentiating Eq. 14.27:

$$(p_u)_{sa} = \gamma H\left[\frac{K_0 H\tan\phi\sin\beta}{\tan(\beta-\phi)\cos\alpha_s} + \frac{\tan\beta}{\tan(\beta-\phi)}(b + H\tan\beta\tan\alpha_s) + K_0 H\tan\beta(\tan\phi\sin\beta - \tan\alpha_s) - K_a b\right] \quad (14.28)$$

Copyrighted Material

Copyright © 2006 John Wiley & Sons Retrieved from: www.knovel.com

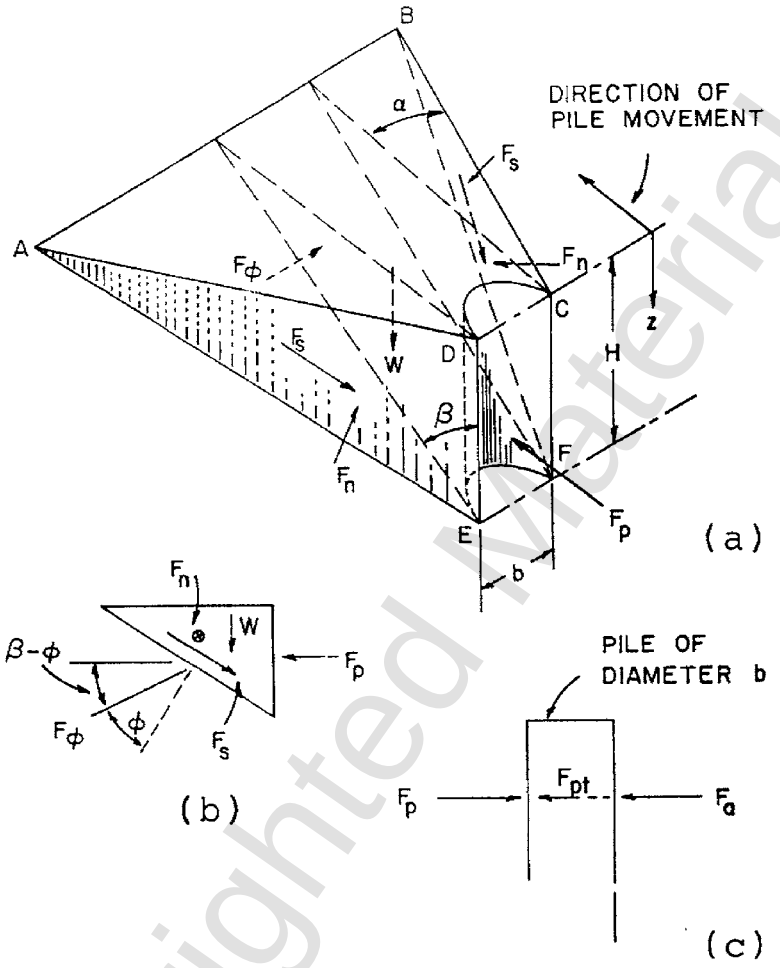

Figure 14.13 Assumed passive wedge-type failure of a pile in sand: (a) general shape of the wedge; (b) forces on the wedge, (c) forces on the pile.

Bowman (1958) performed laboratory experiments with careful measurements and suggested values of α_s ranging from $\phi/3$ to $\phi/2$ for loose sand and up to ϕ for dense sand. The value of β is approximated by the following equation:

$$\beta = 45 + \phi/2 \tag{14.29}$$

The model for computing the ultimate soil resistance at some distance below the ground surface is shown in Figure 14.14a. The stress σ_1 at the back of the pile must be equal to or larger than the minimum active earth pressure; if not, the soil could fail by slumping. The assumption is based on

Copyrighted Material

Copyright © 2006 John Wiley & Sons Retrieved from: www.knovel.com

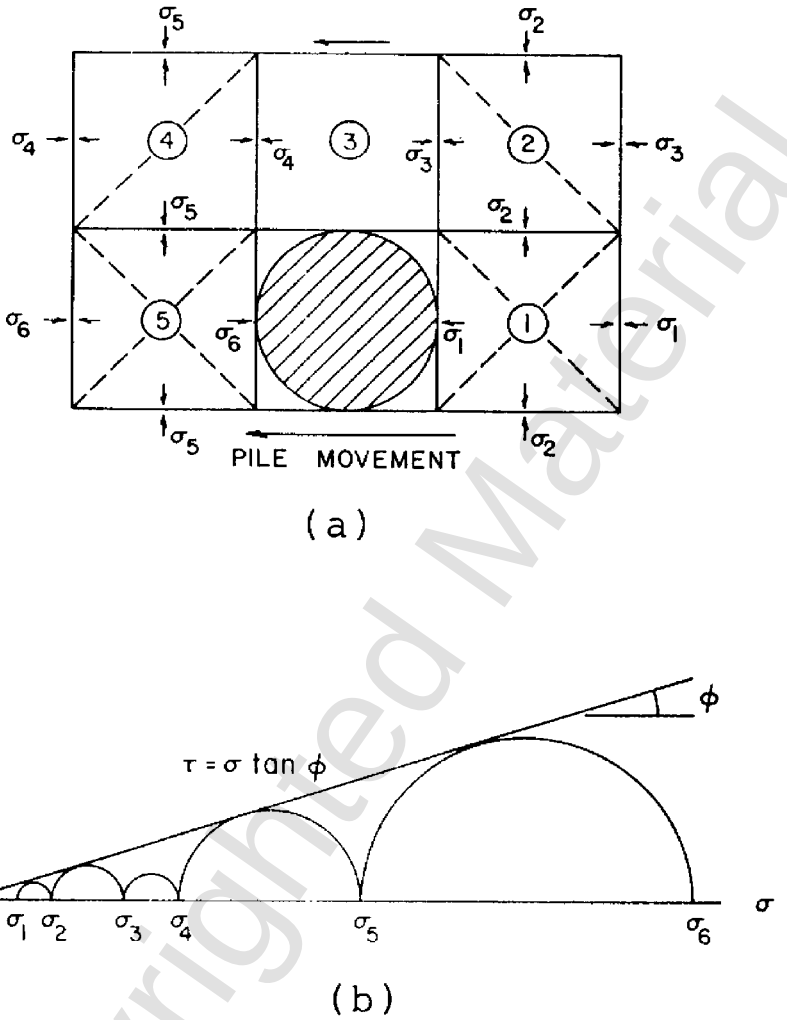

Figure 14.14 Assumed mode of soil failure by lateral flow around a pile in sand: (a) section through the pile; (b) Mohr-Coulomb diagram.

two-dimensional rather than three-dimensional behavior; therefore, some approximation is introduced. If the states of stress shown in Figure 14.14b are assumed, the ultimate soil resistance for horizontal movement of the soil is

$$(p_u)_{sb} = K_A b\gamma H(\tan^8 \beta - 1) + K_0 b\gamma H \tan \phi \tan^4 \beta \qquad (14.30)$$

The equations for $(p_u)_{sa}$ and $(p_u)_{sb}$ are approximate because of the elementary nature of the models used in the computations. However, the equations

Copyrighted Material

Copyright © 2006 John Wiley & Sons Retrieved from: www.knovel.com

serve a useful purpose in indicating the form, if not the magnitude, of the ultimate soil resistance.

Early Recommendations The presentation of the recommendations of Terzaghi (1955) is of interest here, but it is recognized that his coefficients probably are meant to reflect the slope of secants to *p-y* curves rather than the initial moduli. As noted earlier, Terzaghi recommended the use of his coefficients up to the point where the computed soil resistance was equal to about one-half of the ultimate bearing stress. The numerical values given by Terzaghi for E_{py} started correctly with zero at the ground surface and increased linearly with depth, but they are not shown here because the values are for some undetermined points along the *p-y* curves. The recommendations provided a basis for computation, but his values could not be implemented very well until the digital computer became available.

Parker and Reese (1971) performed some small-scale experiments, examined unpublished data, and recommended procedures for predicting *p-y* curves for sand. The method apparently received little use because the method described below, based on a comprehensive testing program, soon became available.

Response of Sand Above and Below the Water Table The recommendations shown here are based principally on an extensive series of tests performed at a site on Mustang Island, near Corpus Christi, Texas (Cox et al., 1974). Two steel-pipe piles, 610 mm (24 in.) in diameter, were driven into sand in such a manner as to simulate the driving of an open-ended pipe and were subjected to lateral loading. The embedded length of the piles was 21 m (69 ft). One of the piles was subjected to short-term loading and the other to repeated loading.

The soil at the site was uniformly graded fine sand with an angle of internal friction of 39°. The submerged unit weight was 10.4 kN/m^3 (66 lb/ft^3). The water surface was maintained at 150 mm (6 in.) or so above the mudline throughout the test program.

The following procedure is for short-term static loading and for cyclic loading and is illustrated in Figure 14.15 (Reese et al., 1974).

1. Obtain values for the friction angle ϕ, the soil unit weight γ, and the pile diameter b (note: use buoyant unit weight for sand below the water table and total unit weight for sand above the water table).
2. Compute the ultimate soil resistance per unit length of pile using the smaller of the values given by the following equations:

$$p_{st} = \gamma z\left[\frac{K_0 \tan\phi \tan\beta}{\tan(\beta-\phi)\cos\alpha} + \frac{\tan\beta}{\tan(\beta-\phi)}(b + z\tan\beta\tan\alpha) + K_0 z\tan\beta(\tan\phi\sin\beta - \tan\alpha) - K_A b\right] \quad (14.31)$$

Copyright © 2006 John Wiley & Sons Retrieved from: www.knovel.com

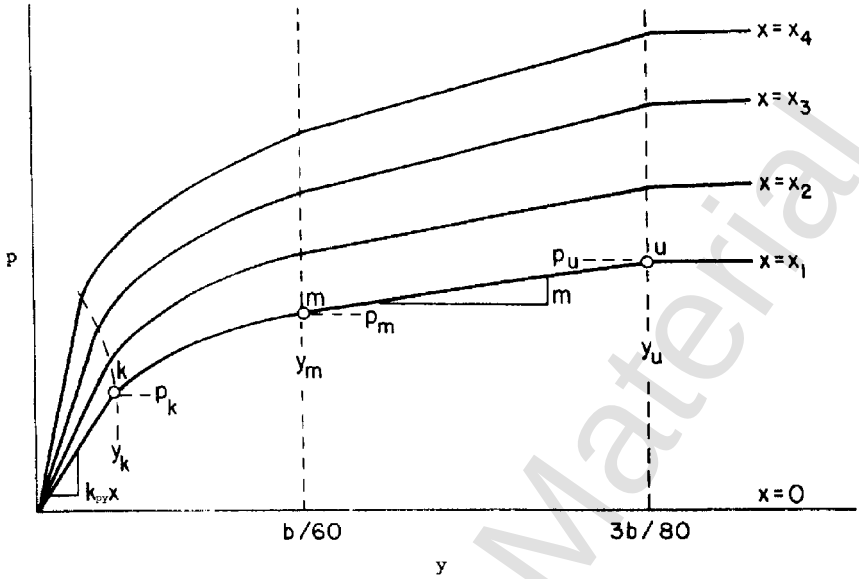

Figure 14.15 Characteristic shape of a family of *p-y* curves for static and cyclic loading in sand.

$$p_{st} = K_A b\gamma z(\tan^8 \beta - 1) + K_0 b\gamma z \tan \phi \tan^4 \beta \qquad (14.32)$$

where $\alpha = \phi/2$.

3. In making the computation in Step 2, find the depth z_t at which there is an intersection at Eqs. 14.31 and 14.32. Above z_t use Eq. 14.31. Below z_t use Eq. 14.32.
4. Select a depth at which a *p-y* curve is desired.
5. Establish y_u as $3b/80$. Compute p_u by the following equation:

$$p_u = \overline{A_s} p_s \quad \text{or} \quad p_u = \overline{A_c} p_s \qquad (14.33)$$

Use the appropriate value of $\overline{A_s}$ or $\overline{A_c}$ from Figure 14.16 for the particular nondimensional depth and for either the static or cyclic case. Use the appropriate equation for p_s, Eq. 14.31 or Eq. 14.32, by referring to the computation in Step 3.

6. Establish y_m as $b/60$. Compute p_m by the following equation:

$$p_m = B_s p_s \quad \text{or} \quad p_m = B_c p_s \qquad (14.34)$$

Use the appropriate value of B_s or B_c from Figure 14.17 for the particular nondimensional depth and for either the static or cyclic case. Use the appropriate equation for p_s. The two straight-line portions of

Copyrighted Material

Copyright © 2006 John Wiley & Sons Retrieved from: www.knovel.com

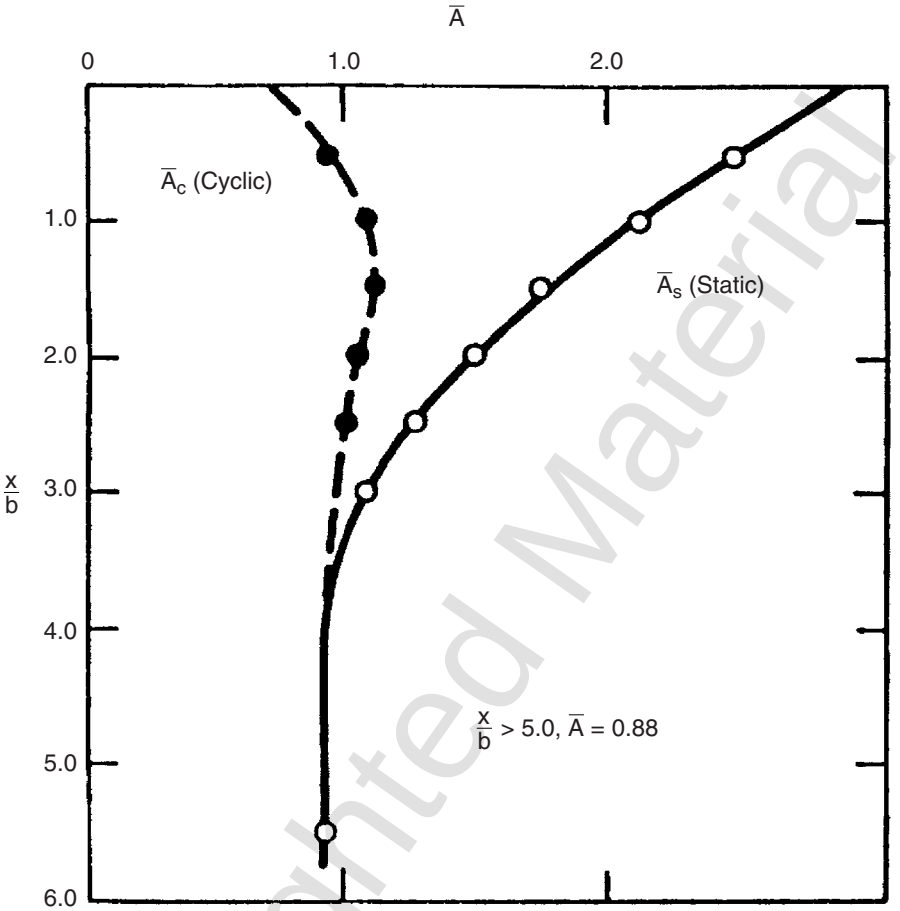

Figure 14.16 Values of coefficients A_c and A_s.

the *p*-*y* curve, beyond the point where y is equal to $b/60$, can now be established.

7. Establish the initial straight-line portion of the *p*-*y* curve:

$$p = K_{py} z y \tag{14.35}$$

Use the appropriate value of K_{py} from Table 14.3.

8. Establish the parabolic section of the *p*-*y* curve:

$$p = \overline{C} y^{1/n} \tag{14.36}$$

Fit the parabola between points k and m as follows:

Copyrighted Material

Copyright © 2006 John Wiley & Sons Retrieved from: www.knovel.com

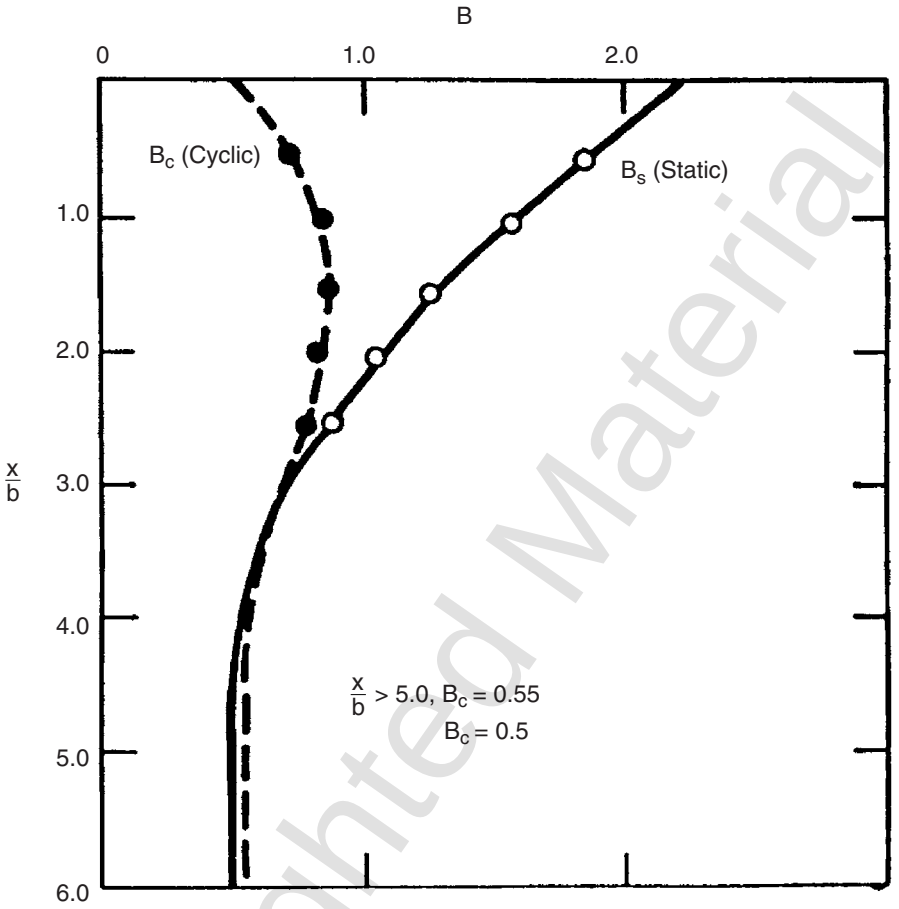

Figure 14.17 Values of coefficients B_c and B_s.

a. Find the slope of the line between points m and u using

$$m = \frac{p_u - p_m}{y_u - y_m} \tag{14.37}$$

b. Obtain the power of the parabolic section using

$$n = \frac{p_m}{m y_m} \tag{14.38}$$

c. Obtain the coefficient as follows:

$$\overline{C} = \frac{p_m}{y_m^{1/n}} \tag{14.39}$$

Copyrighted Material

Copyright © 2006 John Wiley & Sons Retrieved from: www.knovel.com

d. Determine point k as

$$y_k = \left(\frac{\overline{C}}{K_{py}\, z}\right) \tag{14.40}$$

e. Compute the appropriate number of points on the parabola using Eq. 14.36.

Note: The step-by-step procedure is outlined, and Figure 14.15 is drawn, as if there is an intersection between the initial straight-line portion of the *p-y* curve and the parabolic portion of the curve at point *k*. However, in some instances there may be no intersection with the parabola. Equation 14.35 defines the *p-y* curve until there is an intersection with another branch of the *p-y* curve; if no intersection occurs, Eq. 14.35 defines the complete *p-y* curve. This completes the development of the *p-y* curve for the desired depth. Any number of curves can be developed by repeating the above steps for each desired depth.

Triaxial compression tests are recommended for obtaining the friction angle of the sand. Confining pressures close to or equal to those at the depths being considered in the analysis should be used. Tests must be performed to determine the unit weight of the sand. However, it may be impossible to obtain undisturbed samples, and frequently the angle of internal friction is estimated from results of some type of in situ test. The procedure above can be used for sand above the water table if appropriate adjustments are made in the unit weight and angle of internal friction of the sand.

Another method for predicting the *p-y* curves for sand is presented by the API in its manual on recommended practice (RP2A). The two main differences between the recommendations given above and the API recommendations concern the initial slope of the *p-y* curves and the shape of the curves.

The following procedure is for short- term static loading and for cyclic loading as described in API RP2A (1987). The API recommendations were developed only for submerged sand, but the assumption is made that the method can be used for sand both above and below the water table, as was done for the recommendations above.

1. Obtain values for the friction angle ϕ, the soil unit weight γ, and the pile diameter b (note: use buoyant unit weight for sand below the water table and total unit weight for sand above the water table).
2. Compute the ultimate soil resistance at a selected depth z. The ultimate lateral bearing capacity (ultimate lateral resistance p_u) for sand has been found to vary from a value at shallow depths determined by Eq. 14.41 to a value at deep depths determined by Eq. 14.42. At a given depth, the equation giving the smallest value of p_u should be used as the ul-

Copyrighted Material

Copyright © 2006 John Wiley & Sons Retrieved from: www.knovel.com

timate bearing capacity.

$$p_{us} = (C_1 z + C_2 b)\gamma z \tag{14.41}$$

$$p_{ud} = C_3 b \gamma z \tag{14.42}$$

where C_1, C_2, and C_3 are coefficients determined from Figure 14.18.

3. Develop the *p-y* curve based on the ultimate soil resistance p_u, which is the smallest value of p_u calculated in Step 2 and using Eq. 14.43:

$$p = Ap_u \tanh\left(\frac{E_{py\ \max} z}{Ap_u} y\right) \tag{14.43}$$

where $A = 0.9$ for cyclic loading and $\left(3 - 0.8\frac{z}{b}\right) \geq 0.9$ for static loading, and K_{py} is found in Figure 14.19.

14.3.4 Modifications to *p-y* Curves for Sloping Ground

The recommendations for *p-y* curves presented to this point are developed for a horizontal ground surface. To allow designs to be made if a pile is installed on a slope, the *p-y* curves must be modified. The modifications

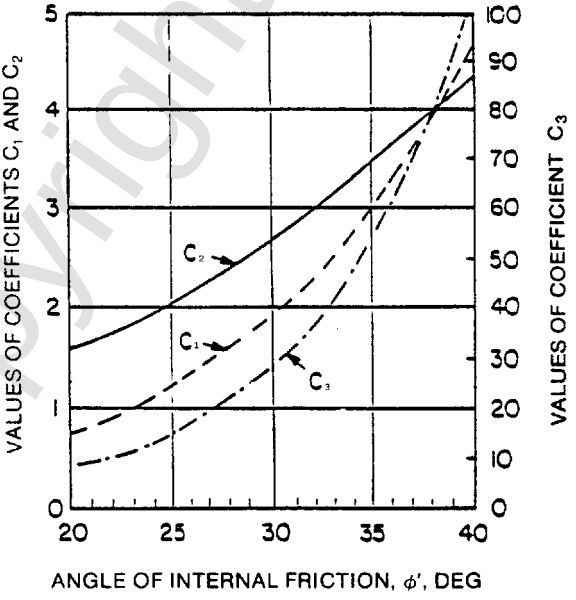

Figure 14.18 Coefficients as a function of Φ'.

Copyrighted Material

Copyright © 2006 John Wiley & Sons Retrieved from: www.knovel.com

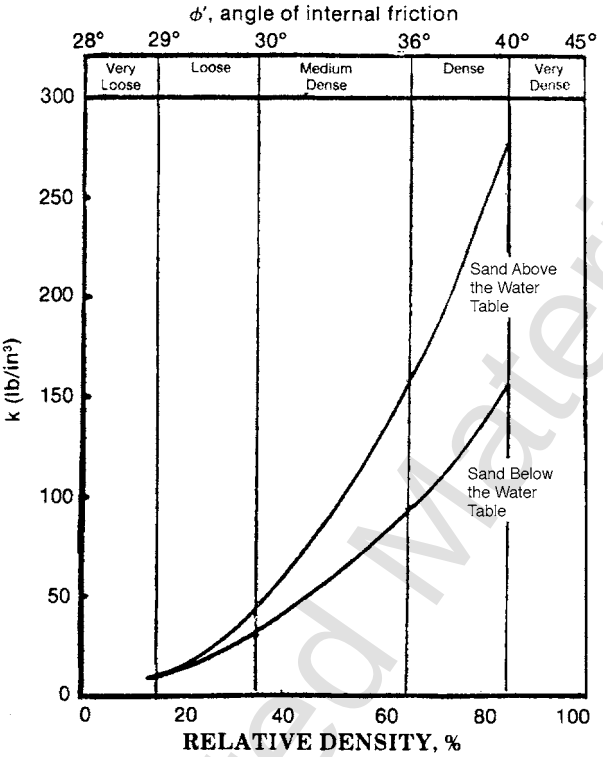

Figure 14.19 Initial modulus of the subgrade reaction, k, used for API sand criteria.

involve revisions in the manner in which the ultimate soil resistance is computed. In this regard, the assumption is made that the flow-around failure will not be influenced by sloping ground; therefore, only the equations for the wedge-type failure need modification.

The solutions presented here are entirely analytical and must be considered preliminary. Additional modifications may be indicated if it is possible to implement an extensive laboratory and field study.

Equations for Ultimate Resistance in Clay The ultimate soil resistance near the ground surface for saturated clay where the pile was installed in ground with a horizontal slope was derived by Reese (1958) and is shown in Eq. 14.44:

$$p_{\text{uca}} = 2c_a b + \gamma bH + 2.83c_a H \tag{14.44}$$

If the ground surface has a slope angle θ, as shown in Figure 14.20, the ultimate soil resistance near the ground surface if the pile is pushed against the downhill slope is

Copyrighted Material

Copyright © 2006 John Wiley & Sons Retrieved from: www.knovel.com

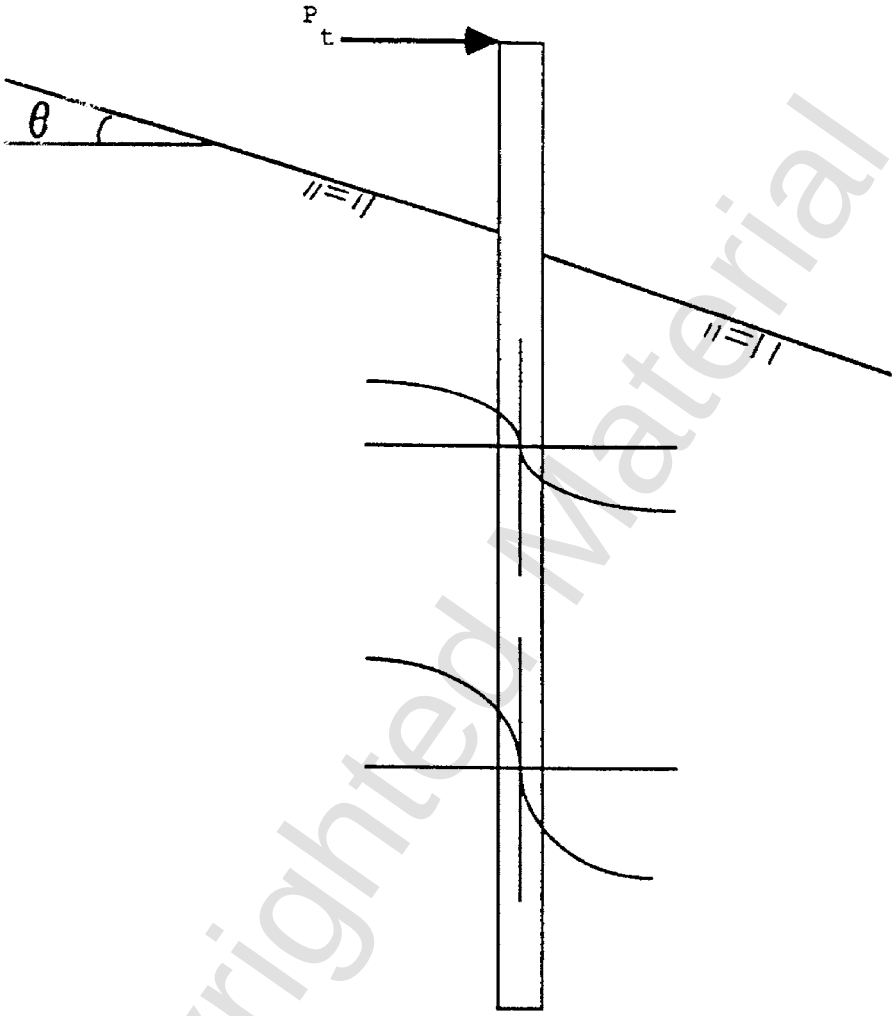

Figure 14.20 Pile installed in sloping ground.

$$p_{\text{uca}} = (2c_a b + \gamma bH + 2.83c_a H)\left(\frac{1}{1 + \tan\theta}\right) \tag{14.45}$$

The ultimate soil resistance near the ground surface if the pile is pushed against the uphill slope is

$$p_{\text{uca}} = (2c_a b + \gamma bH + 2.83c_a H)\left(\frac{\cos\theta}{\sqrt{2}\cos(45 + \theta)}\right) \tag{14.46}$$

where

Copyrighted Material

Copyright © 2006 John Wiley & Sons Retrieved from: www.knovel.com

c_a = average undrained shear strength in the vicinity of the ground surface, and

θ = angle of slope as measured from the horizontal.

A comparison of Eqs. 14.45 and 14.46 shows that the equations are identical except for the last terms in parentheses. If θ is equal to zero, the equations become equal to the original equation.

Equations for Ultimate Resistance in Sand The following equations apply to slopes in sand that are less steep than the friction angle of the sand. The ultimate soil resistance near the ground surface is shown in Eq. 14.31 and forms the basis for the equations shown below. If the pile is pushed against a downhill slope with an angle that is less than the friction angle ϕ, the ultimate soil resistance is

$$p_{\text{usa}} = \gamma H \begin{bmatrix} \dfrac{K_0 H \tan\phi \sin\beta}{\tan(\beta - \phi)\cos\alpha}(4D_1^3 - 3D_1^2 + 1) \\ + \dfrac{\tan\beta}{\tan(\beta - \phi)}(bD_2 + H \tan\beta \tan\alpha D_2^2) \\ + K_0 H \tan\beta(\tan\phi \sin\beta - \tan\alpha) \\ (4D_1^3 + 3D_1^2 + 1) - K_A b \end{bmatrix} \tag{14.47}$$

If the pile is pushed against an uphill slope, the ultimate soil resistance is

$$p_{\text{usa}} = \gamma H \begin{bmatrix} \dfrac{K_0 H \tan\phi \sin\beta}{\tan(\beta - \phi)\cos\alpha}(4D_3^3 - 3D_3^2 + 1) \\ + \dfrac{\tan\beta}{\tan(\beta - \phi)}(bD_4 + H \tan\beta \tan\alpha D_4^2) \\ + K_0 H \tan\beta(\tan\phi \sin\beta - \tan\alpha) \\ (4D_3^3 + 3D_3^2 + 1) - K_A b \end{bmatrix} \tag{14.48}$$

where

$$D_1 = \frac{\tan\beta \tan\theta}{\tan\beta \tan\theta + 1} \tag{14.49}$$

$$D_2 = 1 - D_1 \tag{14.50}$$

Copyrighted Material

Copyright © 2006 John Wiley & Sons Retrieved from: www.knovel.com

$$D_3 = \frac{\tan \beta \tan \theta}{1 - \tan \beta \tan \theta} \tag{14.51}$$

$$D_4 = 1 + D_3 \tag{14.52}$$

and

$$K_A = \cos \theta \frac{\cos \theta - (\cos^2 \theta - \cos^2 \phi)^{0.5}}{\cos \theta + (\cos^2 \theta - \cos^2 \phi)^{0.5}} \tag{14.53}$$

This completes the necessary derivations for modifying the equations for clay and sand to analyze a pile under lateral load in sloping ground.

14.3.5 Modifications for Raked (Battered) Piles

The effect of batter on the behavior of laterally loaded piles was investigated by the use of experiments. The lateral soil-resistance curves for a vertical pile in a horizontal ground surface were modified by a constant to account for the effect of the inclination of the pile. The values of the modifying constant as a function of the batter angle were deduced from the results in the test tank (Awoshika and Reese, 1971) and from the results from full-scale tests (Kubo, 1965). The modifier to be used is shown by the solid line in Figure 14.21.

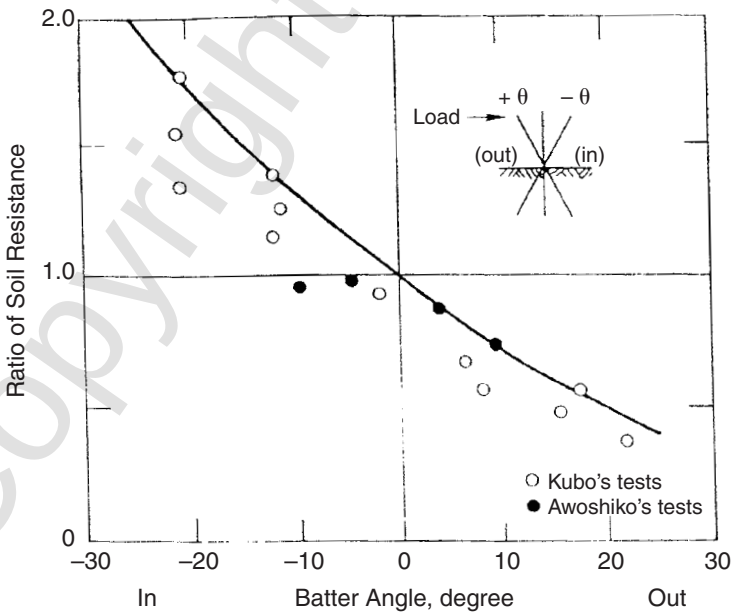

Figure 14.21 Modification of *p-y* curves for battered piles (after Kubo, 1964, and Awoshika and Reese, 1971).

Copyrighted Material

Copyright © 2006 John Wiley & Sons Retrieved from: www.knovel.com

This modifier is to be used to increase or decrease the value of p_u, which in turn will cause each of the p-values to be modified. While it is likely that the value of p_u for the deeper soils is not affected by batter, the behavior of a pile is affected only slightly by the resistance of the deeper soils; therefore, the use of the modifier for all depths is believed to be satisfactory.

As shown in Figure 14.21, the agreement between the empirical curve and the experiments for the out-batter piles (θ is positive) is somewhat better than that for the in-batter piles. The data indicate that the use of the modifier will yield somewhat questionable results; therefore, on an important project, the responsible engineer may wish to recommend full-scale testing.

14.3.6 Recommendations for *p-y* Curves for Rock

Introduction The use of deep foundations in rock is frequently required for support of transmission towers or other structures that sustain lateral loads of significant magnitude. Because the rock must be drilled in order to make the installation, drilled shafts (called *caissons* or *bored piles*) are frequently used. However, a steel pile could be grouted into the drilled hole. In any case, the designer must use appropriate mechanics, as shown elsewhere in this book, to compute the ultimate bending moment and the nonlinear bending stiffness *EI*. Experimental results show conclusively that *EI* must be reduced, as the bending moment increases, to achieve a correct result (Reese, 1997).

In some applications the axial load is negligible, so the penetration is controlled by the lateral load. Computations should be initiated by the designer with a relatively large penetration of the pile into the rock. After a suitable geometric section is found, the factored loads are employed and computer runs are made, with penetration being gradually reduced. The groundline deflection is plotted as a function of penetration, and a penetration is selected that provides adequate security against a sizable deflection of the bottom of the pile.

The following sections present concepts that form the basis for computing the response of piles in rock. The background for designing piles in rock is given and then two sets of criteria are presented, one for strong rock and the other for weak rock.

The secondary structure of rock is an overriding feature with respect to its response to lateral loading. Thus, an excellent subsurface investigation is assumed prior to making any design. The appropriate tools for investigating the rock are employed and the RQD should be obtained, along with the compressive strength of intact specimens. If possible, sufficient data should be taken to allow the computation of the rock mass rating (RMR). Sometimes, the RQD is so low that no specimens can be obtained for compressive tests. The performance of pressuremeter tests in such instances is indicated.

If investigation shows that there are soil-filled joints or cracks in the rock, the procedures suggested here should not be used but full-scale testing at the site is recommended. Furthermore, full-scale testing may be economical if a

Copyrighted Material

Copyright © 2006 John Wiley & Sons Retrieved from: www.knovel.com

large number of piles are to be installed at a particular site. Such field testing will add to the data bank and lead to improvements in the recommendations shown below, which should be considered preliminary because of the meager amount of experimental data available.

In most designs, the deflection of the drilled shaft (or another kind of pile) will be so small that the ultimate strength p_{ur} of the rock is not developed. However, the ultimate resistance of the rock should be predicted to allow computation of the lateral loading that causes the failure of the pile. Contrary to the predictions of *p-y* curves for soil, where the unit weight is a significant parameter, the unit weight of rock is neglected in developing the prediction equations that follow. While a pile may move laterally only a small amount under the working loads, prediction of the early portion of the *p-y* curve is important because the small deflections may be critical in some designs.

Most specimens of intact rock are brittle and will develop shear planes under low amounts of shearing strain. This fact leads to an important concept about intact rock. *The rock is assumed to fracture and lose strength under small values of deflection of a pile*. If the RQD of a stratum of rock is zero or has a low value, the rock is assumed to have already fractured and, thus, will deflect without significant loss of strength. This concept leads to the recommendation of two sets of criteria for rock, one for strong rock and the other for weak rock. In the presentations here, strong rock is assumed to have a compressive strength of 6.9 MPa (1000 psi) or more.

The method for predicting the response of rock is based strongly on a limited number of experiments and on correlations that have been presented in technical literature. Some of the correlations are inexact; for example, if the engineer enters the figure for correlation between stiffness and strength with a value of stiffness from the pressuremeter, the resulting strength can vary by an order of magnitude, depending on the curve that is selected. The inexactness of the necessary correlations, plus the limited amount of data from controlled experiments, means that the methods for the analysis of piles in rock should be used with both judgment and caution.

Field Experiments An instrumented drilled shaft (bored pile) was installed in vuggy limestone in the Florida Keys (Reese and Nyman, 1978) and was tested under lateral loads. The test was performed to gain information for the design of foundations for highway bridges.

Two cores from the site were tested. The undrained shear strengths of the specimens were taken as one-half of the unconfined compressive strength and were 1.67 MPa (17.4 ton/ft^2) and 1.30 MPa (13.6 ton/ft^2). The rock at the site was also investigated by in situ grout-plug tests under the direction of Dr. John Schmertmann (1977). A 140-mm (5.5-in.)-diameter hole was drilled into the limestone, a high-strength steel bar was placed to the bottom of the hole, and a grout plug was cast over the lower end of the bar. The bar was pulled until failure occurred, and the grout was examined to see that failure occurred at the interface of the grout and limestone. The average of the eight

Copyrighted Material

Copyright © 2006 John Wiley & Sons Retrieved from: www.knovel.com

tests was 1.56 MPa (18.3 ton/ft^2). However, the rock was stronger in the zone where the deflections of the drilled shaft were most significant, and a shear strength of 1.72 MPa (18.0 tons/ft^2) was selected for correlation.

The bored pile was 1220 mm (48 in.) in diameter and penetrated 13.3 m (43.7 ft) into the limestone. The overburden of fill was 4.3 m (14 ft) thick and was cased. The load was applied at 3.51 m (11.5 ft) above the limestone. A maximum horizontal load of 667 kN (75 tons) was applied to the pile. The maximum deflection at the point of load application was 18.0 mm (0.71 in.), and at the top of the rock (bottom of the casing) it was 0.54 mm (0.0213 in.). While the load versus deflection curve was nonlinear, there was no indication of rock failure.

The California Department of Transportation (Caltrans) performed lateral-load tests of two drilled shafts (bored piles) near San Francisco (Speer, 1992). The test results, while unpublished, have been provided with the courtesy of Caltrans. Two borings were made into the rock, and sampling was done with a NWD4 core barrel in a cased hole with a diameter of 102 mm (4 in.). The sandstone was medium to fine-grained, with grain sizes ranging from 0.1 to 0.5 mm (0.004 to 0.02 in.), well sorted, and thinly bedded, with a thickness of 25 to 75 mm (1 to 3 in.). Recovery was generally 100%. The reported RQD values ranged from 0 to 80, with an average of 45. Speer (1992) described the sandstone as very intensely to moderately fractured, with bedding joints, joints, and fracture zones.

Pressuremeter tests were performed, and the results were scattered. The values for the moduli of the rock were obtained, and a correlation was employed between the initial stiffness and the compressive strength. Three intervals of rock depth were identified with the following compressive strengths: 0 to 3.9 m, 1.86 MPa; 3.9 to 8.8 m, 6.45 MPa; and below 8.8 m, 16.0 MPa (0 to 12.8 ft, 270 psi; 12.8 to 28.9 ft, 936 psi; and below 28.9 ft, 2320 psi). The strength of the lowest interval is in the strong rock category; however, the first interval is mainly effective in providing the resistance to lateral loading.

Two drilled shafts, 2.25 m (7.38 ft) in diameter, with penetrations of 12.5 m (41 ft) and 13.8 m (45 ft), were tested simultaneously. Lateral loading was accomplished by hydraulic rams, acting on high-strength steel bars that were passed through tubes, transverse and perpendicular to the axes of the piles. Load was measured by load cells, and deflection was measured by transducers. The slope and deflection of the tops of the piles were obtained by readings from the slope indicators.

The load was applied in increments at 1.41 m (4.6 ft) above the ground line for Pile A and 1.24 m (4.1 ft) for Pile B. The pile-head deflection was measured at slightly different points above the rock, but the results were adjusted slightly to yield equivalent values for each of the piles. The load-deflection data for the two piles show that Pile A apparently had a structural weakness, so only Pile B was used in developing the recommendations for *p-y* curves. A groundline deflection of 17 mm was measured at a lateral load

Copyrighted Material

Copyright © 2006 John Wiley & Sons Retrieved from: www.knovel.com

of 8000 kN, but the deflection increased to 50 mm at a lateral load of 8950 kN.

Interim Recommendations for Computing p-y Curves for Weak Rock

The *p-y* curve shown in Figure 14.22 is characteristic of the family representing the behavior of weak rock. The expression for the ultimate resistance p_{ur} for rock is derived from the mechanics for the ultimate resistance of a wedge of rock at its surface:

$$p_{ur} = \alpha_r q_{ur} b\left(1 + 1.4\,\frac{z_r}{b}\right) \quad \text{for} \quad 0 \le z_r \le 3b \tag{14.54}$$

$$p_{ur} = 5.2\alpha_r q_{ur} b \quad \text{for} \quad z_r > 3b \tag{14.55}$$

where

q_{ur} = compressive strength of the rock, usually lower-bound, as a function of depth,
α_r = strength reduction factor b = diameter of the pile, and
z_r = depth below the rock surface.

The assumption is made that failure will occur at the surface of the rock after small deflections of the pile. The compressive strength of intact specimens is reduced by multiplication by α_r to account for fractures in the rock. The value of α_r is assumed to be one-third for an RQD of 100 and to increase linearly to unity at an RQD of 0. The RQD values near the ground surface

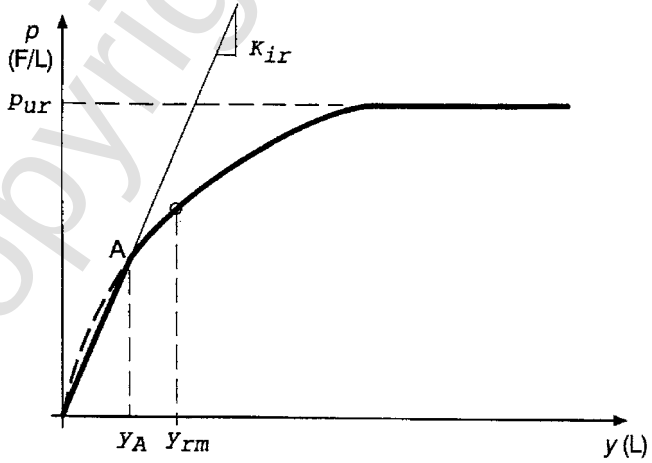

Figure 14.22 Sketch of a *p-y* curve for weak rock (after Reese, 1997).

Copyrighted Material

Copyright © 2006 John Wiley & Sons Retrieved from: www.knovel.com

should be given more weight, taking into account the random nature of the presence of fractures. If RQD is zero, the compressive strength may be obtained directly from a pressuremeter curve, or approximately from Figure 14.23, by entering the value of the pressuremeter modulus.

In considering a strip from a beam resting on an elastic, homogeneous, and isotropic solid, the initial modulus $(E_{py\,\max})_r$ in Figure 14.22 may be shown to have the following value (using the symbols for rock):

$$(E_{py\ \max})_r \cong k_{ir} E_{ir} \tag{14.56}$$

where

k_{ir} = dimensionless constant, and
E_{ir} = initial modulus of the rock.

Equations 14.57 and 14.58 for k_{ir} are derived from experimental data and reflect the assumption that the presence of the rock surface will have a similar effect on k_{ir} as was shown for p_{ur} for ultimate resistance:

$$k_{ir} = \left(100 + \frac{400 z_r}{3b}\right) \quad \text{for} \quad 0 \le z_r \le 3b \tag{14.57}$$

$$k_{ir} = 500 \quad \text{for} \quad z_r \ge 3b \tag{14.58}$$

With guidelines for computing p_{ur} and $(E_{py\,\max})_r$ the equations for the three branches of the family of p-y curves for rock in Figure 14.22 can be computed with the equations that follow.

Branch 1:
$$p = (E_{py\,\max})_r\, y \quad \text{for} \quad y \le y_A \tag{14.59}$$

Branch 2:
$$p = \frac{p_{ur}}{2}\left(\frac{y}{y_m}\right)^{0.25} \quad \text{for} \quad y \le y_A,\ p \le p_{ur} \tag{14.60}$$

and

$$y_{rm} = k_{rm} b \tag{14.61}$$

where k_{rm} = a constant ranging from 0.00005 to 0.0005. The value of y_A is computed by Eq. 14.62:

$$y_A = \left(\frac{p_{ur}}{2(y_m)^{0.25}\, k_{ir}}\right)^{1.333} \tag{14.62}$$

Branch 3:
$$p = p_u \tag{14.63}$$

Copyrighted Material

Copyright © 2006 John Wiley & Sons Retrieved from: www.knovel.com

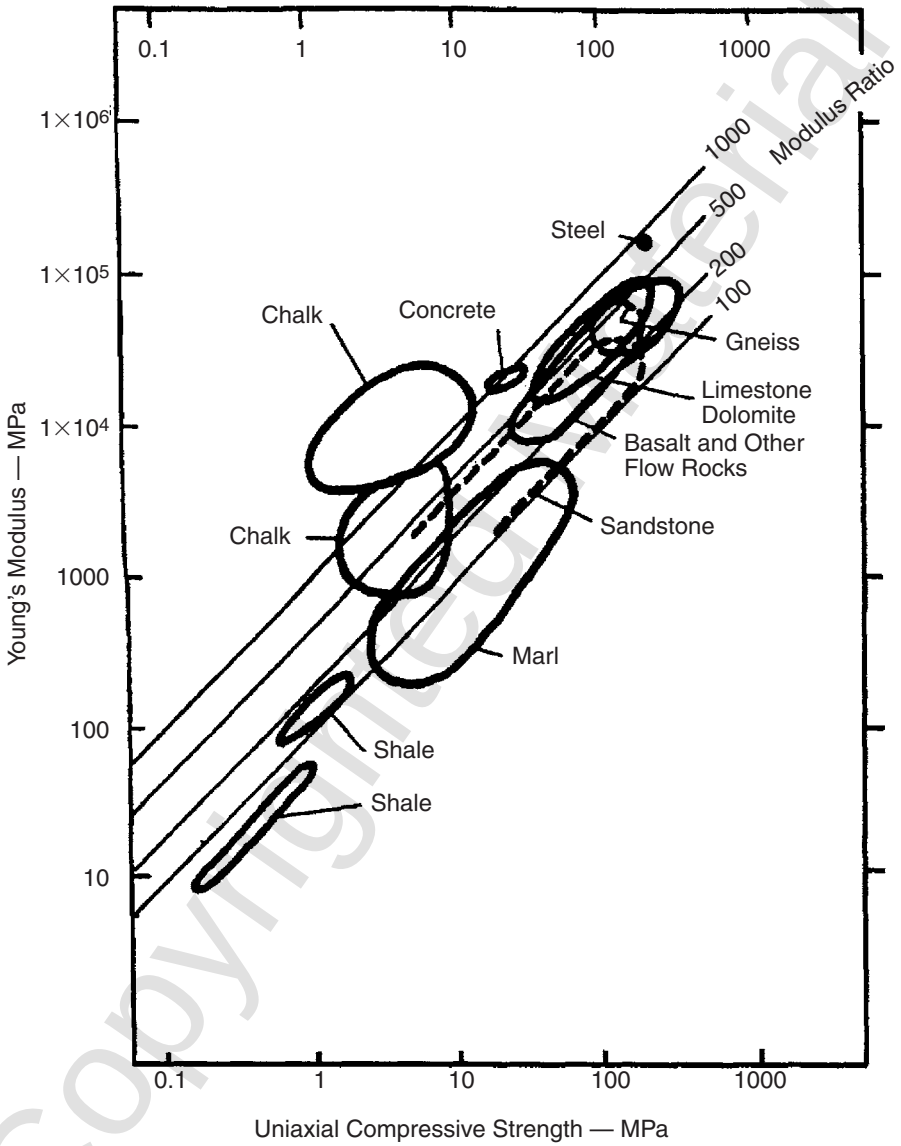

Figure 14.23 Engineering properties of intact rock (after Deere, 1968; Horvath and Kenney, 1979; Peck, 1976).

Copyrighted Material

Copyright © 2006 John Wiley & Sons Retrieved from: www.knovel.com

In selecting a value for k_{rm}, 0.0005 was used to obtain agreement with the experimental results for the test at Islamorada and 0.00005 was used to get agreement between the analytical and experimental results for the test at San Francisco (Reese, 1997). A review of the analyses of the experiments at Islamorada and San Francisco (Reese, 1997) shows that an important parameter is the nonlinear *EI* of the reinforced-concrete section of the drilled shaft. Therefore, computation of the nonlinear *EI* must be given careful attention, and parametric studies can be beneficial in selecting a value of k_{rm}, using a value from the given range to achieve conservatism.

Interim Recommendations for Computing p-y Curves for Strong Rock

The recommendations shown here for strong rock are based on elementary mechanics and on the assumption that there are few cracks and joints in the rock, especially near the rock surface. The *p-y* curve recommended for rock, with compressive strength of intact specimens q_{ur} larger than 6.9 MPa (1000 psi), is shown in Figure 14.24. If the rock increases in strength with depth, the strength at the top of the stratum will normally control. Cyclic loading is assumed to cause no loss of resistance.

As shown in Figure 14.24, load tests are recommended if deflection of the rock (and pile) is greater than $0.0004b$, and brittle fracture is assumed if the lateral stress (force per unit length) against the rock becomes greater than one-half of the diameter times the compressive strength of the rock.

14.4 SOLUTION OF THE DIFFERENTIAL EQUATION BY COMPUTER

14.4.1 Introduction

The limitations imposed on the nondimensional method presented in Chapter 12 are eliminated by the use of finite differences. Some of the capabilities of the method are as follows: a unique *p-y* curve can be input at every increment along the pile; the nonlinear bending stiffness of a reinforced-concrete pile can be input; distributed loading from flowing water or moving soil can be taken into account; the effect of axial loading on bending can be considered explicitly; a variety of boundary conditions at the head and toe of the pile make possible the solution of a variety of practical problems; rapid solutions for a given set of inputs allow the investigation of various parameters and evaluation of various designs; and incrementing of the loading allows the investigation of pile failure by development of a plastic hinge or excessive deflection.

The problems with the finite-difference method are important. Writing the required computer program, using double-precision arithmetic, is complicated, and the available programs must be checked for correctness by the use of standard mechanics; in addition, the engineer must use care in entering the input for a particular problem. Some codes have built-in checks of certain

Copyright © 2006 John Wiley & Sons Retrieved from: www.knovel.com

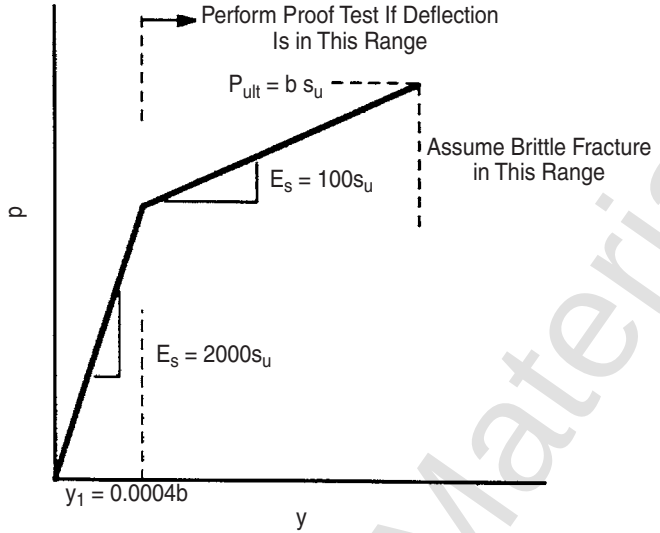

Figure 14.24 Recommended *p-y* curve for strong rock.

parameters to ensure correctness, but most codes require diligence on the part of the engineer.

A good example of necessary diligence involves selection of the number of increments into which the pile is subdivided (see Figure 14.25). Selection of too few increments means errors in solving the differential equation; se-

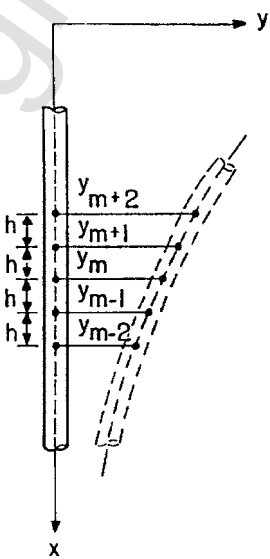

Figure 14.25 Computer representation of a deflected pile.

Copyrighted Material

Copyright © 2006 John Wiley & Sons Retrieved from: www.knovel.com

lection of too many increments leads to an erroneous solution because the difference between successive increments disappears. However, use of the computer program with understanding and care leads to good solutions of many practical problems.

14.4.2 Formulation of the Equation by Finite Differences

With the subdivision of the pile as shown in Figure 14.25, the derivatives can be written in difference form as follows:

$$\frac{dy}{dx} = \frac{y_{m-1} - y_{m+1}}{2h} \tag{14.64}$$

$$\frac{d^2y}{dx^2} = \frac{y_{m-1} - 2y_m + y_{m+1}}{h^2} \tag{14.65}$$

$$\frac{d^3y}{dx^3} = \frac{-y_{m-2} + 2y_{m-1} - 2y_{m+1} + y_{m+2}}{2h^3} \tag{14.66}$$

$$\frac{d^4y}{dx^4} = \frac{y_{m-2} - 4y_{m-1} + 6y_m - 4y_{m+1} + y_{m+2}}{h^4} \tag{14.67}$$

Using the expressions above, and by substitution into Equation 14.1, shown below,

$$E_pI_p \frac{d^4y}{dx^4} + P_x \frac{d^2y}{dx^2} - p + W = 0 \tag{14.1}$$

The differential equation for a pile under lateral loading in difference form is

$$\begin{aligned} &y_{m-2}R_{m-1} + y_{m-1}(-2R_{m-1} - 2R_m + P_xh^2) \\ &+ y_m(R_{m-1} + 4R_m + R_{m+1} - 2P_xh^2 + E_{pym}h^4) \\ &+ y_{m+1}(-2R_m - 2R_{m+1} + P_xh^2) + y_{m+2}R_{m-1}Wh^4 = 0 \end{aligned} \tag{14.68}$$

where $R_m = (E_pI_p)_m$, the bending stiffness of the pile at point m. If a pile is subdivided into n increments, $n + 1$ equations of the form of Eq. 14.68 can be written, leading to $n + 5$ unknowns. The following section shows the formulation of the four needed equations, two at the top of the pile and two at the bottom, to reflect appropriate boundary conditions.

Copyrighted Material

Copyright © 2006 John Wiley & Sons Retrieved from: www.knovel.com

14.4.3 Equations for Boundary Conditions for Useful Solutions

Bottom of the Pile Numbering of the increments along the pile assigns zero to the bottom point, giving the deflection at the bottom as y_0. Then the two imaginary points for use in implementing the boundary conditions are y_{-1} and y_{-2}. Assuming no eccentric axial load at the bottom of the pile, the first of the two boundary conditions sets the moment equal to zero:

$$y_{-1} - 2y_0 + y_1 = 0 \tag{14.69}$$

The second boundary condition needed is for the shear. In most solutions for piles under lateral loading, the pile will experience two or more points of zero deflection, and the deflection at the tip of the pile will be so small that any shear due to pile deflection will be negligible. Thus, the second equation needed is Eq. 14.70:

$$(y_{-2} - 2y_{-1} + 2y_1 - y_2) = 0 \tag{14.70}$$

There may be occasions when the engineer wishes to analyze the behavior of a ''short'' pile where there is only one point of zero deflection along the length of the pile. In that case, the deflection of the bottom of the pile could cause a shearing force to develop. Then Eq. 14.71 would be the second needed equation for the boundary conditions at the bottom of the pile:

$$\frac{R_0}{2h}(y_{-2} - 2y_{-1} + 2y_1 - y_2) = V_0 \tag{14.71}$$

If the engineer can formulate an equation for V_0 as a function of y_0, Eq. 14.71 can be revised to reflect the formulation. If there is a small deflection at the bottom of the pile, the lateral deflection at the top will be larger and could lead to excessive deflection. Designing a pile with only one point of zero deflection would probably be done only if the tip of the pile is founded in rock. The effect on shear of any axial deflection at the bottom of the pile is ignored in Eq. 14.71.

Top of the Pile The top of the pile can experience a number of boundary conditions, as shown in the following sections. Numbering of the increments along the pile assigned the letter t to the top point, giving the deflection at the top of the pile as y_t.

Shear and Moment. If a pile extends above the groundline and a lateral load is applied at its top, the boundary conditions at the groundline are a known moment and a shear. If M_t defines the moment at the top of the pile and P_t

Copyrighted Material

Copyright © 2006 John Wiley & Sons Retrieved from: www.knovel.com

defines the shear (or horizontal load), the two boundary equations for the top of the pile are

$$\frac{R_t}{h^2}(y_{t-1} - 2y_t + y_{t+1}) = M_t \tag{14.72}$$

$$\frac{R_t}{2h^3}(y_{t-2} - 2y_{t-1} + 2y_{t+1} - y_{t+2}) + \frac{P_x}{2h}(y_{t-1} - y_{t+1}) = P_t \tag{14.73}$$

An alternative way to solve the problem of a pile extending above the ground surface is to employ the known lateral load P_t and let M_t equal to zero. The *p-y* curves for the portion of the pile above the groundline can be input to shown zero values of p for all values of y.

Shear and Rotation. The top of a pile may be secured into a thick mat of concrete and essentially fixed against rotation. In other designs, the rotation of the top of the pile may be known or estimated. In both instances, the lateral load (shear) is assumed to be known. The following equation may be used with Eq. 14.73 for the boundary conditions at the top of the pile, where S_t is the rotation of the top of the pile:

$$\frac{y_{t-1} - y_{t+1}}{2h} = S_t \tag{14.74}$$

Shear and Rotational Restraint. There are occasions when the top of a pile is extended and becomes part of the superstructure. In the construction of an offshore platform, for example, a prefabricated template is set on the ocean floor and extends above the water surface. Piles are stabbed into open vertical pipes comprising the legs of the platform and then driven to a predetermined depth. Spacers or grout are used in the annular space between the template leg and the pile, allowing the rotational restraint at the pile head below the template to be computed by structural analysis. There may be other constructions where the rotational restraint at the pile head may be known or estimated. The following equation, along with Eq. 14.73, may be used for the boundary conditions at the top of the pile:

$$\frac{\dfrac{R_t}{h^2}(y_{t-1} - 2y_t + y_{t+1})}{\dfrac{y_{t-1} - y_{t+1}}{2h}} = \frac{M_t}{S_t} \tag{14.75}$$

Moment and Deflection. An example of the use of this boundary condition is when a pile supports a bridge abutment. The pile head is not restrained against rotation, leading to a zero moment at the pile head, but the lateral

Copyrighted Material

Copyright © 2006 John Wiley & Sons Retrieved from: www.knovel.com

deflection Y_t at the pile head is known or can be estimated. In other instances, the pile-head moment may be known or estimated. The following equation, along with Eq. 14.72, can be used for the boundary conditions at the top of the pile:

$$y_t = Y_t \tag{14.76}$$

Deflection and Rotation. When a pile supports a superstructure, the structural engineer may compute a deflection and a rotation (slope) at the pile head. In that case, Eqs. 14.74 and 14.76 may be used for the boundary conditions.

14.5 IMPLEMENTATION OF COMPUTER CODE

A number of computer codes have been written both in the United States and abroad, and have been augmented from time to time, utilizing the equations and procedures presented here. The code used in the computations that follow is LPILE©, and a CD-ROM containing a Student Version of LPILE is included on the inside of the back cover of this book. Many of the computations shown below can be run with the Student Version of LPILE.

The form of the results from a solution with LPILE is shown in Figure 14.26. The deflection along the lower portion of the pile is exaggerated to illustrate the fact that the deflection oscillates, with decreasing values, from positive to negative over the full length of the pile consistent with input. The curves are related mathematically. For example, the values of p are negative when y is positive, and p and y are zero at the same points along the pile.

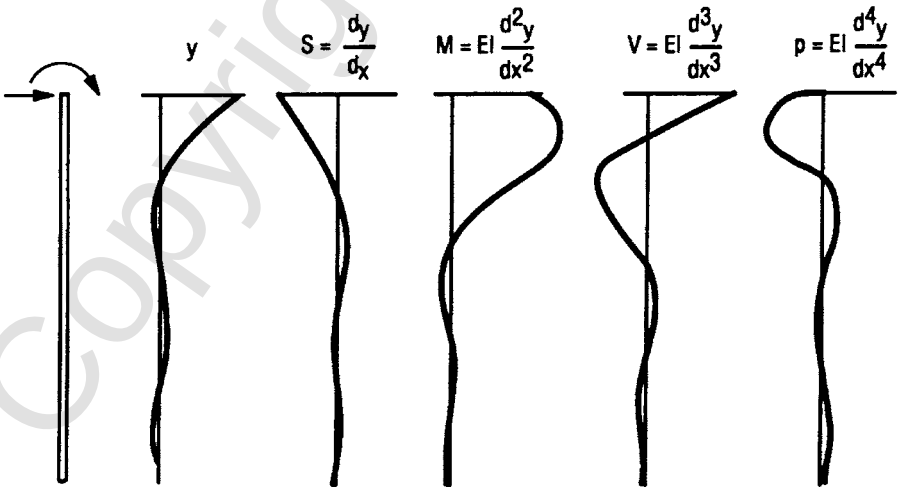

Figure 14.26 Form of the results obtained from a complete solution with LPILE.

Copyrighted Material

Copyright © 2006 John Wiley & Sons Retrieved from: www.knovel.com

The solution of the difference equations for behavior of a particular pile under lateral loading must be solved by iteration because the soil response is a nonlinear function of pile deflection. The computer code begins with an arbitrary set of values for E_{py} and solves for a set of deflections along the length of the pile such as shown in Figure 14.26. The *p*-*y* curves are employed and new values of E_{py} are obtained and a new set of *y*-values is computed. The new values of *y* are compared with the previous set and the solution continues until convergence occurs where all values of *y* for the present computation are within a given tolerance of the values of *y* in the just previous solution. The tolerance is set at a very small value of deflection to ensure an accurate solution of the difference equations.

14.5.1 Selection of the Length of the Increment

As shown in Figure 14.24 and in Eq. 14.68, the length of the increment between points along the pile where difference equations are written, as noted earlier, is an important parameter affecting the accuracy of a solution. A study is shown here to illustrate the importance of selecting an appropriate length for *h*. A steel-pipe pile with a diameter of 380 mm, used in a computation in Chapter 12, was selected for the study. The moment of inertia *I* was $4.414 \times 10^{-4}\ m^4$, the modulus of elasticity *E* of the steel was 2.0×10^8 kPa, and the yield strength of the steel was 250,000 kPa. Loading was selected for the pile to cause a significant deflection while keeping the bending stress below the yield point of the steel.

The computations are made for the case of a constant value of E_{py} for which a closed-form solution (Hetenyi, 1946) exists that will yield a precise result to compare with the output from the computer code. Comparison will be made of the pile-head deflection from the ''exact'' solution and the computer solution where the value of the increment length is changed through a wide range. The equations for the closed-form solution for deflection along the pile are

$$y = \frac{e^{-\beta x}}{2E_p I_p \beta^2}\left[\frac{P_t}{\beta}\cos\beta x + M_t(\cos\beta x - \sin\beta x)\right] \tag{14.77}$$

$$\beta = \left(\frac{E_{py}}{4E_p I_p}\right)^{1/4} \tag{14.78}$$

The equations are for a pile of infinite length, but Timoshenko (1941) pointed out that the solution is valid where the nondimensional length of the pile (βL) is equal to or greater than 4. For the solutions with the computer code, $P_t = 40$ kN, $M_t = 0$, and $E_{py} = 100\ \text{kN/m}^2$, entered as constant along the length of a pile with a length of 40 m. In order to make computations to compare with the closed-form solution, the value of E_{py} was entered by im-

Copyrighted Material

Copyright © 2006 John Wiley & Sons Retrieved from: www.knovel.com

plementing the numerical feature of the *p-y* curves with one linear curve at the top of the pile and the same curve at the bottom of the pile. The value of β was computed to be 0.129724, yielding a value of $\beta L = 5.2$.

The closed-form solution yielded a value of y_t of 0.103779 m. The computer code allowed the user to enter a number of increments from 40 to 300. The results from the computer were (no. of increments, y_t, m): 40, 0.103365; 60, 0.103607; 80, 0.103692; 100, 0.103731; 150, 0.103770; 200, 0.103783; 250, 0.103790; and 300, 0.103365. All of the computer values agreed with the closed-form solution for three places. The greatest error was the result from 40 increments, where the computed value was less than the closed-form value by 0.000414 m, an acceptable accuracy in view of the uncertainties in the input for most solutions. The greatest accuracy occurred for increments of 150 through 300, and the least accuracy occurred for an increment of 40.

However, if the pile length is increased from 40 m while maintaining the increments at 40, errors become significant. The results from the computer were (pile length m, y_tm): 60, 0.102801; 100, 0.101087; 150, 0.097831; 200, 0.093489; 250, 0.088301; and 300, 0.082571. None of the solutions is acceptable, and serious errors occur if the pile is subdivided too grossly. For a length of 300 m and for 40 increments, the length of an increment is 7.5 m, far too much to allow a correct depiction of the curved shape of the pile. Significant errors can occur, for example, if the length of the pile is relatively great because of axial loading and the same length is used for analysis of the response to lateral loading. The output should be examined, and the length for lateral analysis should be reduced if zero deflection is indicated more than three or four times.

A rule of thumb that seems to have some merit is to select an increment length of about one-half of the pile diameter. Using this approach, the number of increments for a pile length of 50 m in the first computations would be about 200. The specific data that were selected for the comparison between a closed-form solution show acceptable accuracy regardless of the number of increments selected, from 40 to 300, as allowed by the particular code. However, if the length of an increment becomes too great with respect to the diameter of a pile, significant errors will result. The user is urged to repeat the study shown here for piles with other dimensions.

14.5.2 Safe Penetration of Pile with No Axial Load

The design of a pile subjected only to lateral loading is required on occasion, and the engineer must determine the minimum penetration that is safe against excessive deflection. Problems will occur, particularly as the pile sustains cyclic loads, when there is one point of zero deflection and the tip of the pile deflects. The pile used in the above example will be used in the following study. The pile, loading, and resistance remain as before, and the length of the pile is reduced to examine its response. The length of the increment was made about one-half of the pile diameter.

Copyright © 2006 John Wiley & Sons Retrieved from: www.knovel.com

The deflection at the top of the pile was unchanged, with a penetration of 30 m where there were just two points of zero deflection. Note that the computer runs were successfully completed as the penetration was decreased by increments of 5 m to a penetration of 10 m. However, the pile-head deflection increased by 60% and the tip of the pile had a deflection of 0.077 m, opposite in direction to that of the pile head. Thus, pile penetrations of less than 30 m for the example were unacceptable for the given data.

This example and the one directly above show that the results from the computer solution must be studied with care to ensure correctness.

14.5.3 Buckling of a Pipe Pile Extending Above the Groundline

The pile used in the above two studies will be used to study the prediction of buckling due to axial load. The pile was assumed to extend 5 m above the ground surface, and two loading conditions were investigated: a lateral load of 1.0 kN applied at the top of the pile and a lateral load of 10.0 kN at the top. Axial loading was increased in increments, and the pile-head deflection was noted in order to predict the load at which buckling would occur.

The pile was assumed to be installed in a stiff clay above the water table with the following properties: undrained shear strength, 75 kPa; total unit weight, 19.0 kN/m^3; K_{py}, 135 MN/m^3; and ε_{50}, 0.005. The results of the computations are shown in Figure 14.27. The amount of lateral load caused a significant effect on the load to cause buckling. While the application of such a pile under a large axial load is unusual, the application of the computer code is of interest and may be of practical use.

14.5.4 Steel Pile Supporting a Retaining Wall

The lateral load sustained by a retaining wall is due principally to active forces behind the wall, with possibly some amount being due to a moving vehicle operating close to the top of the wall. The forces have little cyclic component, so the formulation of *p-y* curves for static loading is appropriate. A single vertical pile is analyzed and is assumed to be far enough from other piles that no interaction occurs due to close spacing.

The pile being analyzed is an H-section with bending about the strong axis. Data from the AISC handbook for the section shows the width of the pile as 373 mm, the depth as 351 mm, the moment of inertia about the *x*-axis as 3.76×10^{-4} m^4, and the yield strength of the steel as 276 MPa. The tabulated modulus at yielding of the steel is 2.39×10^{-3} m^3, giving a value of the bending moment at which a plastic hinge would develop of 660 kN-m. The cross-sectional area of the section is 1.69×10^{-2} m^2, and the modulus of elasticity of the steel is 2×10^8 kPa. In the computer analysis, the pile was assumed to have a diameter of 373 mm. The penetration of the pile below the ground line was 15 m. The pile is assumed to extend about the ground surface and to be embedded in a concrete footing.

Copyrighted material

Copyright © 2006 John Wiley & Sons Retrieved from: www.knovel.com

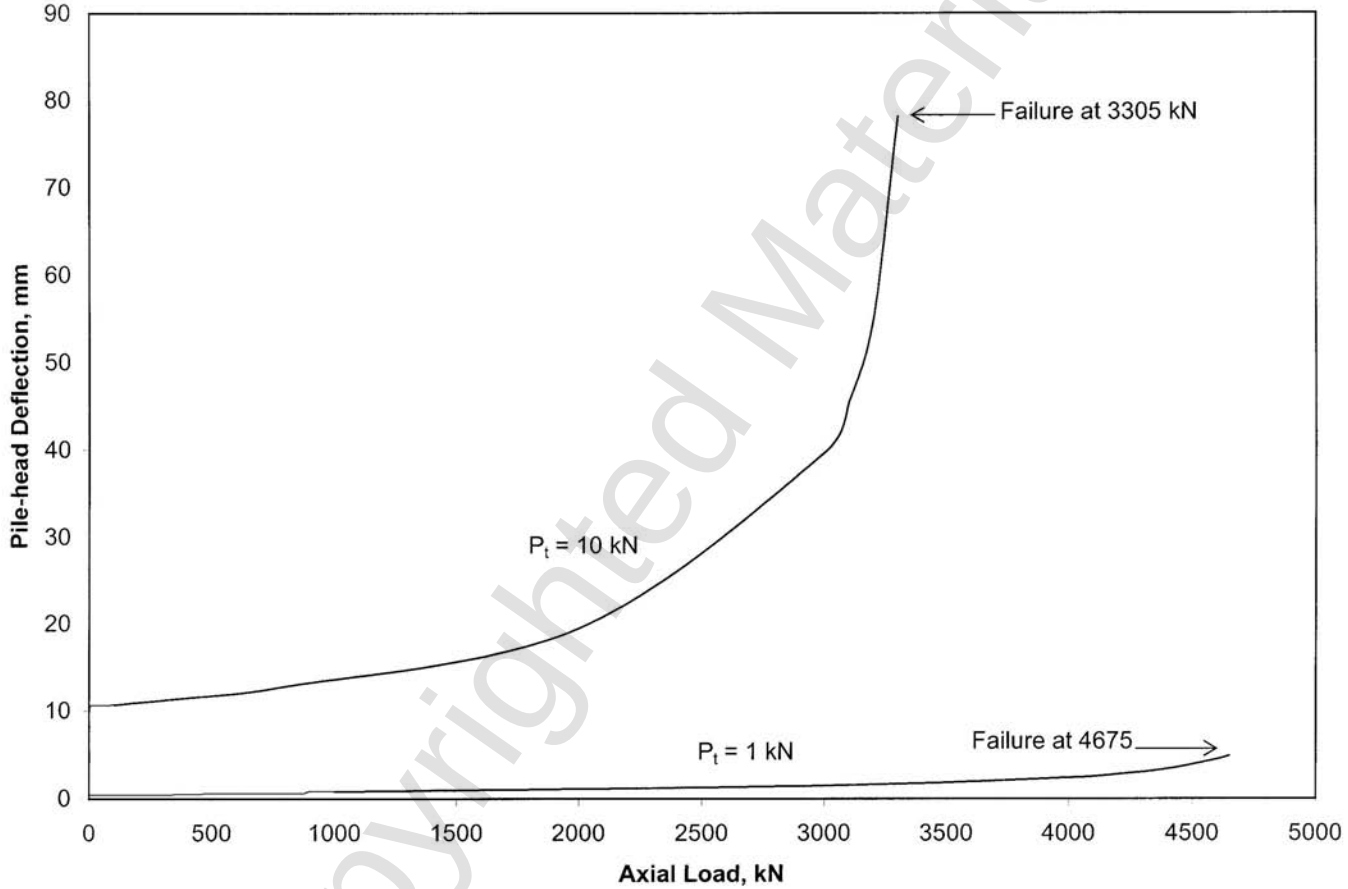

Figure 14.27 Buckling of a pile with 5 m of unsupported length and lateral load at the top.

Copyright © 2006 John Wiley & Sons Retrieved from: www.knovel.com

The soil at the site is a stiff clay above the water table with the following properties: $\gamma = 18.7$ kN/m^3, $c = 96.5$ kPa, and $\varepsilon_{50} = 0.007$. The data from a soil exploration invariably reveal scatter in the properties of the soil. In many cases, lower-bound and upper-bound solutions are desirable, taking into account the range in soil properties and possibly in the possible magnitude of the loadings. Under service conditions, the lateral load of the pile was 175 kN and the axial load was 90 kN.

Two conditions for the rotational restraint at the top of the pile were selected: the pile head was free to rotate (free head), and the pile head was entirely restrained against rotation (fixed head). The results of computations in Table 14.4 show the incrementing of the service load to find the loading at which a plastic hinge would develop. The pile-head deflection was also computed in the belief that the engineer could limit the loading if the deflection was considered excessive.

Table 14.4 shows that, for the free-head case, a plastic hinge developed at a lateral load of 426 kN, or for a load factor of 426/175 = 2.43. For the fixed-head case, a plastic hinge developed at a lateral load of 435 kN, or for a load factor of 435/175 = 2.49. Either of these load factors is acceptable for most designs. The pile-head deflection for the free-head case at the failure load was computed to be 98.3 mm, and for the fixed-head case it was computed to be only 23.4 mm. While the load factor at yield of the steel is about the same for both cases of pile-head rotation, the significant reduction in pile-head deflection for the fixed-head case could indicate special treatment in the design of the pile head support. Achieving full or partial fixity of a pile head is usually accomplished by extending the pile into a stiff pile cap for a distance of perhaps three pile diameters.

Table 14.4 shows the results for loading *above* what would cause a plastic hinge, which are incorrect because a constant *EI* was selected in computation. The improvements can be made if the non-linear *EI* vs. moment curve is

TABLE 14.4 Summary of the Ground Line Deflection and the Maximum Moment Under Different Lateral and Axial Loads for Both Cases of Pile-Head Fixity

	Lateral Load (kN)	Axial Load (kN)	Groundline Deflection (mm)	Maximum Moment (kN-m)
Free head	175	90	15.2	191.3
	350	180	65.1	503.5
	426	219	98.3	664.0
	525	270	157.0	907.1
Fixed head	175	90	3.6	188.0
	350	180	15.0	484.0
	435	224	23.4	652.0
	525	270	34.5	842.0

Copyright © 2006 John Wiley & Sons Retrieved from: www.knovel.com

specified, and the code will indicate the development of a plastic hinge under excessive loadings. The erroneous results are shown here to alert the user to develop a full understanding of the input and output from computer solutions.

The bending-moment curves and pile-deflection curves, as a function of length along the pile, for both cases of pile-head fixity are shown in Figure 14.28. A number of interesting observations can be made. Considering the behavior of the pile under lateral loading, the bottom few meters of the pile are subjected to very little moment or deflection, suggesting that parametric studies could lead to a reduction in the length of the pile unless length is controlled by axial loading.

Also, in both cases, the portion of the pile where the bending moment is largest is relatively small compared to the length of the pile. If the pile consists of reinforced concrete or of a steel pile, the bending strength of the pile can be tailored to agree with the moment curve, perhaps leading to significant savings.

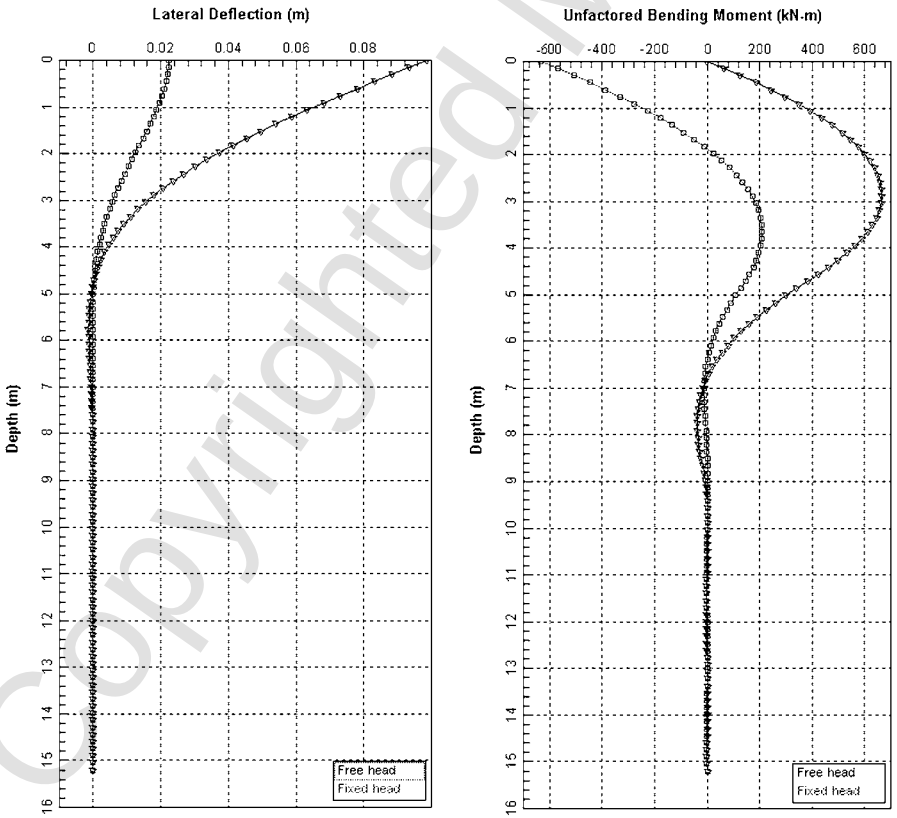

Figure 14.28 Pile-deflection curves and bending moment curves as a function of length along the pile for both cases of pile-head fixity.

Copyrighted Material

Copyright © 2006 John Wiley & Sons Retrieved from: www.knovel.com

The maximum negative moment for the fixed head occurs at the top of the pile and is over three times as large as the maximum positive moment at a depth of about 3.6 m. If the designer is able to allow some rotation of the pile head between fixed and free, the maximum negative moment and the maximum positive moment may be made close to equal, allowing the pile to sustain more lateral load before a plastic hinge develops.

14.5.5 Drilled Shaft Supporting an Overhead Structure

Many towers are being installed that transmit a shear and a moment to the groundline. Such towers are used for transmission lines, microwave supports, wind farms, advertising signs, and highway signs. Drilled shafts (bored piles) are frequently used for the foundation. Drilled shafts have the advantage that a wide variety of soils and rocks can be drilled. Further, using pile-drilling equipment, a geotechnical engineer at the site could arrange a program of rapid in situ testing. In addition, during the drilling of the production pile, the character and strength of the soil or rock could be logged by the engineer. The following paragraphs show how the engineer, with knowledge of the loadings on the overhead structure, could do preliminary computations for expected soil profiles, go to the site with a laptop, and complete the computations after obtaining information on the subsurface conditions.

While most designs are based on a soil boring, for structures requiring a single drilled shaft, a design can be based on soil properties from available geology and from information gained during the preliminary drilling. Loadings will be known from the nature of the structure and the environmental conditions, so a qualified engineer could go to a new site with a laptop and make the final design on site. Using the loadings, the maximum bending moment will occur within a diameter or two from the ground surface, regardless of the strength of the soil, so the required diameter of bending strength of the drilled shaft can be known fairly well at the outset.

A pile was selected for analysis with a diameter of 760 mm and reinforced with 12 vertical rebars with a diameter of 25 mm, spaced equally on a 610-mm-diameter circle that gave a clear space outside the steel of 76 mm. The ultimate strength of the reinforcing steel was 414 MPa, and that of the concrete was 27.6 MPa. The ultimate bending moment of the pile section was computed by the LPILE program as a function of the applied axial load, as shown in Figure 14.29. As may be seen, the axial load has a significant effect on the ultimate bending moment.

The axial load of the column and the superstructure were computed carefully and found to be 222 kN, yielding an ultimate bending moment of 734 m-kN, as shown in the figure. The resultant of the lateral load on the structure was due principally to forces from wind, assumed to be applied at 13 m above the groundline. The axial load will be maintained at 222 kN, which is conservative, as shown in the figure. Using that axial load, the bending stiffness for the section was computed as a function of the applied moment. The results

Copyright © 2006 John Wiley & Sons Retrieved from: www.knovel.com

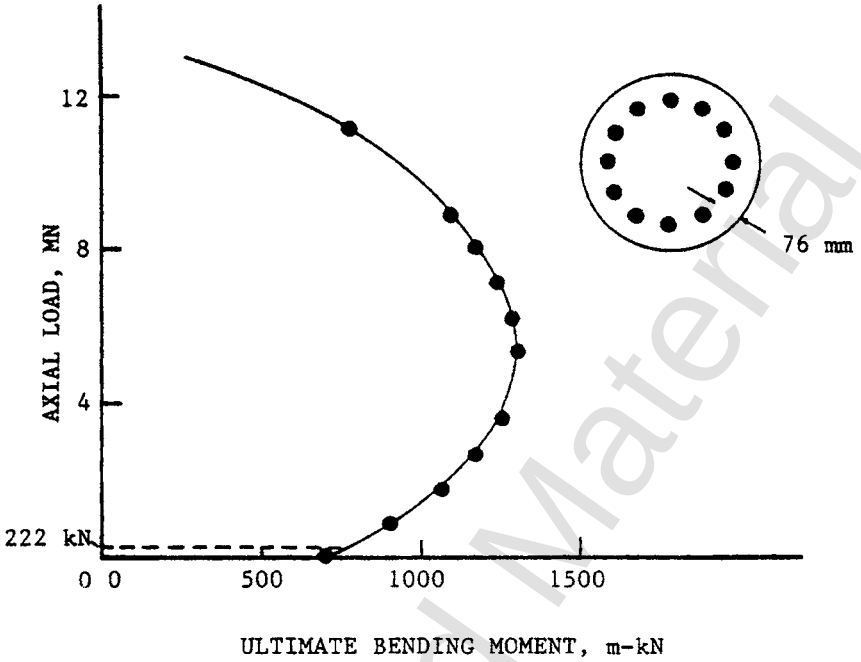

Figure 14.29 Interaction diagram for the drilled shaft of an example problem.

are shown in Figure 14.30. The figure shows a sharp decrease in E_pI_p when cracking of the concrete first occurs. For a range in bending moments, the E_pI_p value is relatively uniform until a significant decrease in E_pI_p occurs prior to the development of a plastic hinge. For the initial analyses, an E_pI_p value of 130,000 kN-m^2 was selected with the idea that the distribution of bending moments along the pile would be reviewed and adjustments made in E_pI_p if required. Alternatively, the computations could be made with a code that selected E_pI_p automatically as a function of the computed bending moment.

The problem is to compute the load required to cause a plastic hinge if the pile is founded above the water table in uniform sand or in overconsolidated clay. The sand has a friction angle of 36°, a total unit weight of 19.5 $\frac{kN}{m^3}$, and $E_{py\,\max}$ of 24 $\frac{MN}{m^3}$. The clay has a undrained shear strength of 75 kPa, a total unit weight of 19.0 $\frac{kN}{m^3}$, an ε_{50} of 0.005, and $E_{py\,\max}$ of 135 $\frac{MN}{m^3}$. Wind gusts will cause cyclic loading, and 200 was selected as the number of cycles to be used in the analysis with the clay. Cyclic loading with sand assumes that there are enough cycles to cause the limiting resistance.

Copyrighted Material

Copyright © 2006 John Wiley & Sons Retrieved from: www.knovel.com

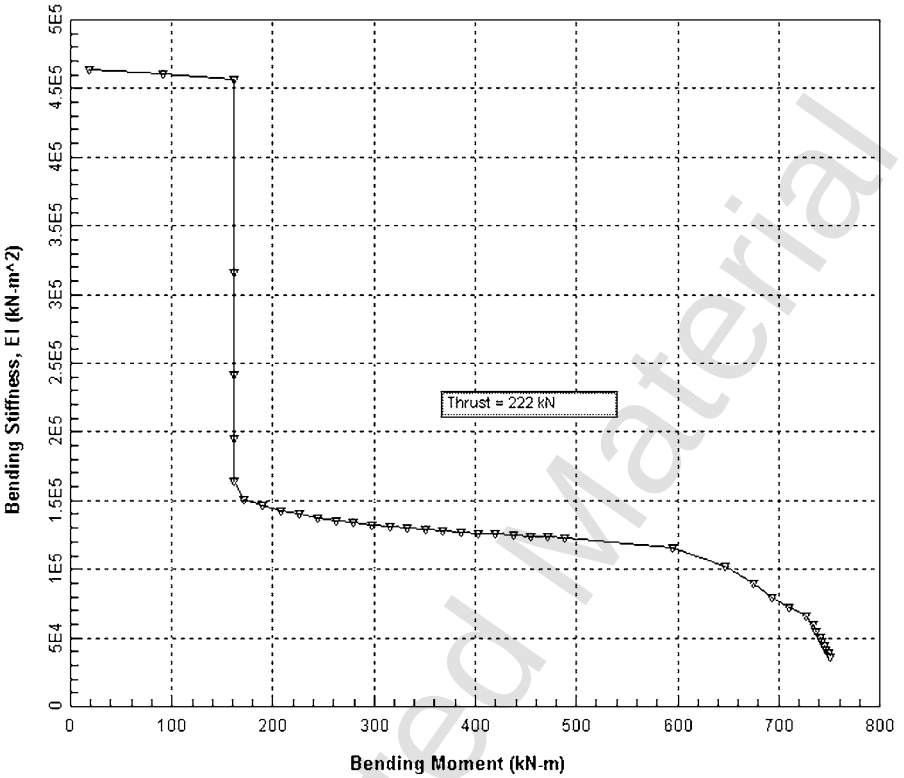

Figure 14.30 Computed values of bending stiffness (*EI*) under an axial load of 222 kN.

The first analysis was done assuming the pile to be installed in sand. The penetration of the pile was selected as 30 m to ensure *long-pile* behavior. The LPILE program was used, with a loading to cause a plastic hinge at the maximum bending moment of 734 m-kN. The lateral load at a height of 13.0 m was found to be 52.9 kN, yielding a moment at the groundline of 687.7 m-kN. The groundline deflection was 29.8 mm. The penetration of the pile was decreased in increments until the number of points of zero deflection was two or three. At a penetration of 10 m, the data showed almost three points of zero deflection. In regard to penetration, the engineer should err on the conservative side to ensure no significant deflection of the tip of the pile.

The bending moment over the length, using the above loading to cause pile failure, showed that about 2 m of the top of the pile showed a bending moment of more than 600 m-kN and about 3 m of the bottom of the pile showed a bending moment of less than 150 m-kN. No attempt was made to correct the E_pI_p values to improve the solution. However, the lateral load at 13 m was factored downward by 2.5, perhaps yielding the service load, and

Copyrighted Material

Copyright © 2006 John Wiley & Sons Retrieved from: www.knovel.com

no moment along the pile exceeded 500 m-kN. Therefore, the use of 130,000 kN-m^2 for E_pI_p was judged to be satisfactory or somewhat conservative at the service load. The deflection at the groundline under this service load was computed to be 9 mm.

The analysis of the pile in clay showed that the maximum bending moment of 734 m-kN was developed by a lateral load of 55.1 kN at 13 m above the groundline, yielding a moment at the ground line of 716.3 m-kN. The deflection of the pile head was 30.9 mm. The penetration of the pile was reduced from 30 m to 8 m where more than 2 points of zero deflection were observed. The loads were reduced by a factor of 2.5 and the bending moment, as for the sand, was in the range to achieve some conservatism. The pile-head deflection at the service load was computed to be less than 10 mm.

The above analyses show that preliminary computation for a given pile with a given set of loadings can be done using a computer code, and a body of information can be developed that will provide guidance to a geotechnical engineer who may go with the drilling contractor to make final computations for the soil that exists at the site.

PROBLEMS

P14.1. Use the Student Version of the LPILE computer program to solve the following problem:

The pile is a steel pipe with an outside diameter of 30 in. (0.76 m) and a wall thickness of 1.0 in. (25.4 mm), cross-sectional area of 91.1 in.^{2} (0.0588 m^2), moment of inertia of 9589 in.^{4} (3.99×10^{-3} m^4), modulus of elasticity 29,000,000 psi (200,000,000 kPa), and yield strength of steel 36,000 psi (248,000 kPa).

The soil is a normally consolidated clay under water with 15 ft (4.6 m) of erosion. Properties at the ground surface: undrained shear strength of 173 psf (8.28 kPa), submerged unit weight of 39.1 lb/ft^3 (6.14 kN/m^3), ε_{50} of 0,02, and K_{py} of 90 lb/in.^{3} (24.4 MN/m^3). Properties at a depth of 85 ft (25.9 m): undrained shear strength 1100 psf (52.6 kPa), submerged unit weight 47.6 lb/ft^3 (7.48 kN/m^3), ε_{50} of 0.02, and K_{py} of 500 lb/in.^{3} (135.7 MN/m^3).

Apply a series of loads P_t at the top of the pile (M_t is zero, P_x is zero) with a pile length of 85 ft; the number of increments along the pile is 100 (the increment length is less than one-half of the pile diameter).

a. Use static loading, with loads increasing in increments of 10 kips to a total of 80 kips (the program will accept the entry of a number of inputs for the loading).

b. Use the Graphics feature of the program to print a plot of maximum bending moment versus applied load and explain the reason

Copyrighted Material

Copyright © 2006 John Wiley & Sons Retrieved from: www.knovel.com

for the curvature in the plot. (Note: the entry for k in the input is K_{py}; use an average value over the depth of 85 ft.)

P14.2. Use the plot from Problem P14.1 to find the lateral load causing a bending stress of 15 ksi, noting that a series of runs can be made with the same entries around the correct value. (An answer within 1% of the precise value is acceptable.)

P14.3. Find a computer solution for the lateral load obtained in Problem P14.1b, print the tabulated output, and plot curves for deflection and soil reaction, both as a function of depth.

a. What penetration should the pile have so that it behaves as a ''long'' pile?

b. Make computations to check the agreement between deflection and soil resistance at ground surface and at a depth of 21.25 ft (255 in.).

P14.4. A free-standing pile is frequently used as a breasting dolphin to protect a dock or pier against damage from a docking vessel. The energy from the docking vessel may be a complex function of many factors. The following equation may be useful:

$$E = 0.5mv^2$$

where E = energy, m = mass of the vessel, and v = velocity on touching the breasting dolphin.

Because docking will occur many times, cyclic loading on the soil should be used. The problem is to compute the energy that can be sustained by the pile in Problem P14.1 if the vessel contacts the pile at 15 ft above the mudline. The maximum bending stress should not exceed 20 kips/in.^{2}.

a. Find the force that will act on the vessel if the given stress is not exceeded.

b. The breasting dolphins should be observed for performance. If locked-in deflection is observed, what steps can be taken to alleviate the problem?

c. Assuming that the vessel will contact two breasting dolphins and that the docking velocity will be 0.5 ft/sec, find the weight of a vessel that can dock without auxiliary fendering.

P14.5. Figure 14.31 shows a portion of an offshore platform. One leg of the jacket or template is shown. The jacket is fabricated on shore and placed in position by a derrick barge. Mud mats can be placed below the bottom braces to prevent the jacket from sinking below the mudline. Piles are stabbed through the jacket legs and driven with a swinging hammer. As shown, spacers welded inside the jacket serve to

Copyrighted Material

Copyright © 2006 John Wiley & Sons Retrieved from: www.knovel.com

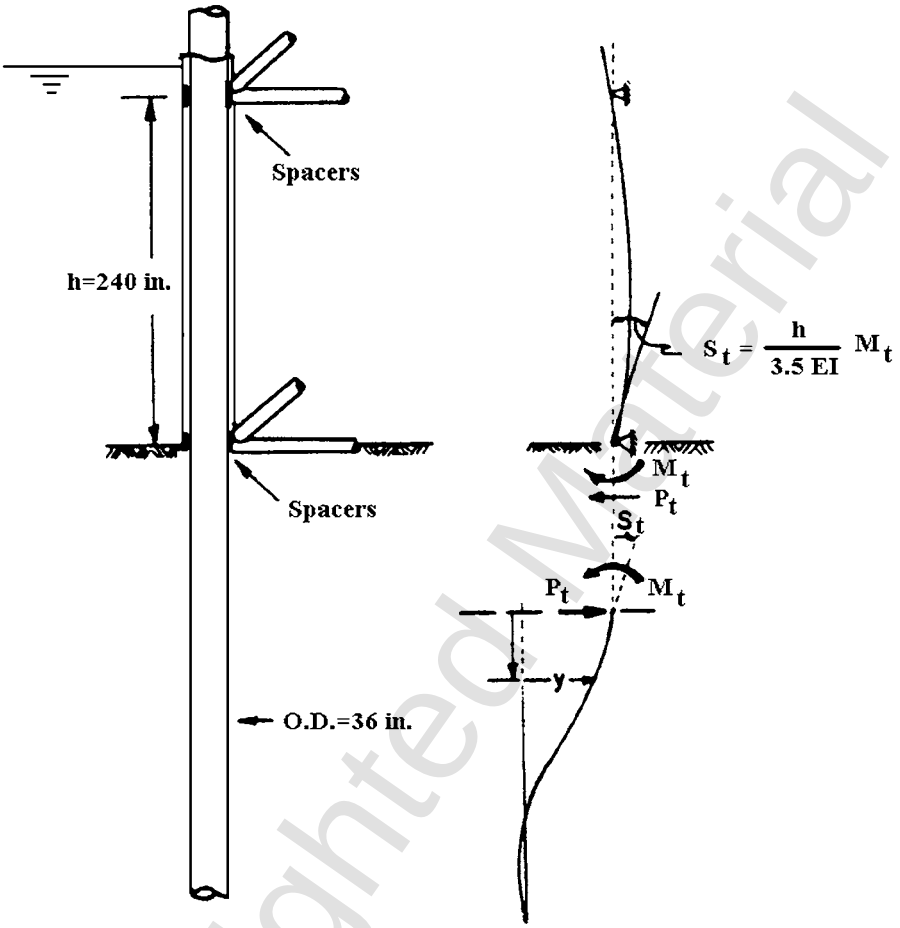

Figure 14.31

center the pile and allow it to rotate at the panel points. Alternatively, if the designer chooses, the annular space between the jacket and pile can be grouted. Both jacket and piles extend above the water surface. A deck section, with legs that extend through the zone of the maximum wave, is placed by a derrick barge and the joints are welded.

During a storm, wave forces, perhaps large, will act against the jacket and cause the structure to move laterally and rotate slightly; the piles must be analyzed by the GROUP computer program (see Chapter 15). A preliminary analysis, however, can be worthwhile even if the jacket rotation is temporarily ignored.

As shown in the free body in Figure 14.31, the pile is partially restrained against rotation. A moment at the pile head will cause a

Copyrighted Material

Copyright © 2006 John Wiley & Sons Retrieved from: www.knovel.com

rotation that must be equal to the rotation of the pile within the jacket that acts as a continuous beam. In the absence of a detailed structural analysis, the end of the pile at the first panel point above the mudline is neither fixed nor free. Therefore, the ratio of moment to rotation can be given by the equation shown in the figure.

The pile has a diameter of 36 in., and the wall thickness in the zone of maximum bending moment is 1.5 in. To save money, the wall thickness can be reduced in steps to an amount that will not be damaged during pile driving. For analysis under lateral loading, a constant wall thickness can be assumed without error. The moment of inertia of the pile is 24,230 in.^{4} (0.01009 m^4), the cross-sectional area is 162.6 in.^{2} (0.105 m^4), the combined stress at failure is 36,000 lb/in.^{2} (248,000 kPa), and the modulus of elasticity is 29×10^6 lb/in.^{2} (2×10^8 kPa).

The pile is installed in a uniformly graded sand with a friction angle of 39°, a relative density of about 0.9, and a submerged unit weight of 66.3 lb/ft^3 (10.4 kN/m^3). The loading will be applied by wave forces that build up gradually with time. The maximum wave forces are usually used in design even though the number of such waves may be limited. Cyclic loading will be selected in developing the *p-y* curves for the sand.

The pile is assumed to penetrate 120 ft into the sand and to develop sufficient axial capacity so that any failure will be due to lateral loading. A load of 500 kips is assumed from the dead weight of the structure and will increase by a factor of 2 times the lateral load due to overturning forces.

a. Find the lateral load on this single pile at which the combined stress of the steel, 36,000 lb/in.^{2} (248,000 kPa), will be developed.

b. If the maximum negative moment and the maximum positive moment are considerably different, investigate the possibility of bringing the two moments closer to each other with increased capacity in loading.

c. Present a brief discussion of how a factor of safety should be developed for the pile.

Copyrighted Material

Copyright © 2006 John Wiley & Sons Retrieved from: www.knovel.com